Soft Tissue Thickness and Composition surrounding the Proximal Femur

by

Alyssa Marie Tondat

A thesis
presented to the University of Waterloo
in fulfillment of the
thesis requirement for the degree of
Master of Science
in
Kinesiology

Waterloo, Ontario, Canada, 2023

Author's Declaration

I hereby declare that I am the sole author of this thesis. This is a true copy of the thesis, including any required final revisions, as accepted by my examiners.

I understand that my thesis may be made electronically available to the public.

Acknowledgements

Abstract

Introduction: In Canada, approximately 30 000 hip fractures occur each year. Hip fractures are associated with significant morbidity, mortality, and quality of life changes. Trochanteric soft tissues have been shown to influence hip fracture risk by absorbing and dissipating energy during sideways falls onto the hip. However, previous research on the relationship between soft tissues and hip fracture has only considered the bulk thickness of the tissues without consideration of the differing contributions of muscle and subcutaneous adipose tissue to total thickness. In addition, despite evidence that the principle impact sites are distal to the greater trochanter (GT), the overwhelming focus has been on the soft tissues directly overlying the GT. Towards improved understanding of impact dynamics (and hip fracture risk), greater knowledge of soft tissue composition and spatial distribution surrounding the proximal femur is necessary.

Objectives and Hypotheses: The first objective is to assess the reliability of ultrasound methods to characterize soft tissue thickness and composition from multiple locations around the lateral proximal femur. The second objective is to provide insights into soft tissue thickness and composition from multiple locations around the lateral proximal femur. It is hypothesized that: 1) intra-rater reliability will be good to excellent (ICC > 0.75) for all soft tissue thickness measurements; 2) intra-rater reliability will differ between measurement locations, with reliability being lower for measurements on the anterolateral and posterolateral femur compared to the lateral femur; 3) there will be a main effect of sex on all soft tissue thickness measurements; 4) there will be a main effect of measurement location on all soft tissue thickness measurements.

Methods: 25 healthy young adults (12 males, 13 females) aged 18 – 35 years old with self-reported BMI ≤ 24.9 kg/m^2 were recruited. B-mode ultrasound (GE LOGIQ E10 ultrasound machine with a L2-9VN-D probe) was used to take measurements of total soft tissue thickness, muscle thickness, and subcutaneous adipose tissue thickness on participant's right hip and femur at 6 cm intervals throughout a 3 x 4 grid centered over the GT. To simulate a lateral fall, participants lay on their right side with their hips and knees straight on a specially designed table with a cut-out to allow for ultrasound imaging of the side of the femur that would impact the ground. Three ultrasound images were taken at each measurement location. Initial analysis was conducted on the 12 separate locations. Following this, thickness measurements from P1 – P4 were averaged together, L1 – L4 were averaged together, and A1 – A4 were averaged together to form posterolateral, lateral, and anterolateral groups.

Two-way mixed effects absolute agreement intraclass correlation models (ICC 3,1) and 95% confidence intervals were used to assess intra-rater reliability across the 12 locations and three tissue types. A two-way mixed model ANOVA with sex as a between groups factor and measurement location (12 locations) as a within groups factor was used to assess differences in soft tissue thickness. A follow up two-way mixed model ANOVA with sex as a between groups factor and measurement location (3 locations) was then conducted to examine differences in soft tissue thickness over areas of the femur that are more representative of fall direction and orientation.

Results: ICCs were good to excellent (ICC > 0.75) for all tissue types and locations, except for muscle thickness and total thickness at A1 and P1. ICCs for muscle thickness were 0.486 at A1 and 0.593 at P1. ICCs for total thickness were 0.56 at A1 and 0.583 at P1. Intra-rater reliability was significantly lower at these locations for these tissues than other locations based on overlap between confidence intervals. There were significant main effects of sex and location across the 12 individual measurement locations for all tissue types (all $p < 0.05$). When grouping the locations together, there was an ordinal interaction between sex and measurement location for total soft tissue thickness ($F = 4.229$, $p = 0.021$) and significant main effects of sex and measurement location for all three tissue types (all $p < 0.05$). Males have significantly more muscle, more total soft tissues, and less adipose than females. Muscle thickness was largest over the anterolateral femur and smallest over the lateral femur, with significant differences between all three locations (all $p < 0.05$). Adipose thickness was largest over the posterolateral femur and smallest over the anterolateral femur, with significant differences between all three locations (all $p < 0.05$). Total soft tissues were significantly lower over the lateral femur compared to the posterolateral and anterolateral femur ($p < 0.001$), with no significant difference in thickness between the posterolateral and anterolateral femur ($p = 1.0$).

Discussion and Conclusion: Results highlight that this ultrasound protocol can be used to reliably measure tissue-specific thicknesses over the proximal femur, except for muscle and total thickness at A1 and P1 locations. The results also show that tissue-specific thicknesses vary across locations over the proximal femur, and with sex. Accordingly, it is important to consider the soft tissues surrounding the GT, the differing contributions of muscle and adipose tissues to total soft tissue thickness, and sex when developing both models of hip fracture risk (from an epidemiological perspective) and mechanical models of hip fracture (from a biomechanical tissue loading perspective).

Table of Contents

List of Figures

List of Tables

List of Abbreviations

AT: Adipose tissue thickness

BMD: Bone mineral density

BMI: Body mass index

CI: Confidence interval

CT: Computed tomography

DXA: Dual energy x-ray absorptiometry

FE: Finite element

FOR: Factor of risk

GT: Greater trochanter

ICC: Intraclass correlation coefficient

MD: Minimum difference to be considered real

MT: Muscle thickness

SEM: Standard error of the measurement

TST: Total soft tissue thickness

TSTT: Trochanteric soft tissue thickness

Chapter 1
Thesis Overview

Falls are the most common cause of injury in older adults, with 20 – 30% of older adults falling each year (Public Health Agency of Canada, 2014). Hip fractures in older adults are a fall-related injury, with 95% of hip fractures in this population being caused by falls (Scott, Wagar, & Elliot, 2010). In Canada, this amounts to approximately 30 000 hip fractures each year (Leslie et al., 2009), with hip fracture risk being highest for lateral falls and sideways landing configurations (Nankaku, Kanzaki, Tsuboyama, & Nakamura, 2005; Yang et al., 2020). Hip fractures are associated with significant morbidity, mortality, and quality of life changes (Adachi et al., 2001; Nazrun, Tzar, Mokhtar, & Mohamed, 2014). The economic burden of hip fractures is huge, with estimated direct costs to Canadians of $1.1 billion per year (Nikitovic, Wodchis, Krahn, & Cadarette, 2013). Accordingly, it is crucial to understand the factors that influence lateral fall-related hip fracture risk to improve hip fracture models and prevention techniques.

Understanding hip fractures and the factors that influence hip fracture risk can be challenging due to our limited ability to study them in-vivo. Experimental studies with human participants are limited by the risk of injury to participants and results from cadaveric studies may not be directly applicable to the living population due to post-mortem changes in tested specimens. Accordingly, models of fall-induced hip fracture become crucial for understanding the mechanisms behind hip fracture, factors that influence hip fracture risk, and the development of effective prevention/intervention techniques. In order for models of hip fracture to provide robust outputs, the inputs to the model must be biofidelic. Research conducted using hip fracture models recognizes the importance of incorporating soft tissues, which have been shown to absorb and dissipate energy during an impact (Majumder, S., Roychowdhury, & Pal, 2013; Robinovitch, McMahon, & Hayes, 1995) and account for the force attenuation that is provided by trochanteric soft tissues during impact (Bachmann et al., 2014; Bhattacharya, Altai, Qasim, & Viceconti, 2019; Bouxsein et al., 2007; Dufour et al., 2012; Fleps et al., 2018; Fleps, Guy, Ferguson, Cripton, & Helgason, 2019; Galliker, Laing, Ferguson, Helgason, & Fleps, 2022; Lafleur, Benoit R., Tondat, Pretty, Mourtzakis, & Laing, 2021; Majumder, S., Roychowdhury, & Pal, 2008; Majumder, S. et al., 2013; Majumder, Santanu, Roychowdhury, & Pal, 2007; Martel, Daniel R., Lysy, & Laing, 2020; Nasiri & Luo, 2016; Nielson et al., 2009; Roberts, Thrall, Muller, & Bouxsein, 2010; Sarvi & Luo, 2015). However, soft tissues (and soft tissue thickness) are currently considered as one bulk tissue/bulk tissue thickness without consideration for

the differing contributions of muscle and subcutaneous adipose tissue to total thickness. In addition, the focus has been on the soft tissues lying directly over the greater trochanter (GT), despite evidence that peak impact forces and peak pressure during sideways falls are located distal and posterior to the GT (Pretty, Steven P., Levine, & Laing, 2021b; Pretty, Steven P., Levine, & Laing, 2021a). To improve our understanding of impact dynamics and hip fracture risk, and to generate more robust hip fracture models, research into soft tissue composition (i.e. muscle vs. subcutaneous adipose tissue) and the spatial distribution of these tissues over the proximal femur is required. Accordingly, this thesis has two main objectives: 1) To provide insights into soft tissue thickness and composition over multiple locations on the proximal femur; and 2) To provide insights into the reliability of ultrasound methods to characterize soft tissue thickness and composition over the proximal femur. Figure 1-1 provides a visual depiction of the framework of this thesis. Specific hypotheses can be found in section 2.6 of this thesis.

Research Questions
1. What is intra-rater reliability of ultrasound thickness measurements?
2. Does intra-rater reliability differ between measurement locations?
3. Are there differences in thickness measurements based on sex and location?

Independent Variables
- Measurement Location
- Sex

Dependent Variables
- Total soft tissue thickness (TST)
- Muscle thickness (MT)
- Subcutaneous adipose thickness (AT)

Participants
- 15 males
- 15 females

Methods
- B-mode Ultrasound

Measurement Location
- 12 locations surrounding proximal femur

Sex
- Male
- Female

TST MT AT

TST MT AT

Reliability Analysis
- Intraclass Correlation Coefficients

Difference Assessments
- Two-way mixed model ANOVAs

Figure 1-1: Visual depiction of the framework of this thesis.

Chapter 2
Literature Review

2.1 Fall-Related Hip Fractures

2.1.1 Prevalence of Fall-Related Hip Fractures

Falls are the most common cause of injury in adults over the age of 65, with 20 – 30% of older adults falling each year (Public Health Agency of Canada, 2014). Falls in older adults lead to 61% of injury deaths and 81% of injury hospitalizations (Parachute, 2021; Public Health Agency of Canada, 2014). In addition to being the leading cause of injury, falls are also the cause of 95% of hip fractures in older adults (Scott et al., 2010). In Canada, this amounts to approximately 30 000 hip fractures each year (Leslie et al., 2009). The high number of hip fractures in older adults places a large economic and social burden on the Canadian population.

2.1.2 The Burden of Fall-Related Hip Fractures

The economic burden of fall-related injuries is huge, costing an estimated $5.6 billion per year and $15.3 million per day (Parachute, 2021). Of these costs, hip fractures are estimated to cost Canadians $1.1 billion per year in direct costs (Nikitovic et al., 2013). When indirect costs are factored into the estimate, the cost of hip fractures in Canada increases to $3.9 billion per year (Tarride et al., 2012). With the large economic burden of hip fractures, it is important to understand the factors that influence hip fracture risk so that appropriate interventions can be developed and implemented.

In addition to being an economic burden on society, fall-related hip fractures also create a significant social impact. They are associated with significant morbidity, mortality, and quality of life changes (Adachi et al., 2001; Nazrun et al., 2014). Following a hip fracture, an individual's risk of future fracture increases three-fold compared to individuals who have no previous fracture, and their risk of death within one year is two times greater than those without hip fracture (Empana, Dargent-Molina, Bréart, & EPIDOS Group, 2004; Nazrun et al., 2014)**.** Additionally, older adults may experience a loss of independence following a hip fracture, with 30% of community dwelling older adults being institutionalized within a year of hip fracture, 30% of hip fracture patients requiring rehab, 18% requiring complex care, and more than 65% of hip fracture patients requiring home care (Morin et al., 2012; Nikitovic et al., 2013). With the large social and economic burden associated with hip fractures, understanding the factors which lead to hip fracture in older adults is crucial. Understanding the risk

4

factors for hip fracture will lead to improved methods for reducing hip fracture risk and preventing hip fractures. In particular, understanding the factors that influence lateral fall-related hip fracture risk is crucial to improving hip fracture models and prevention techniques.

2.1.3 Risk Factors for Hip Fracture

Hip fractures in older adults are fall-related injuries, with several factors influencing hip fracture risk. Hip fracture risk is highest for lateral falls and sideways landing configurations (Nankaku et al., 2005; Yang et al., 2020). Nankaku and colleagues (2005) investigated hip fracture risk during lateral, posterolateral, and posterior falls in human volunteers. They found that while impact forces were highest during posterior falls, hip fracture risk is highest during lateral and posterolateral falls due to more direct impact to the femur. The differences in impact forces and hip fracture risk between fall configurations highlights the potential influence of force attenuation by soft tissues on hip fracture risk. However, more research is needed to better understand how soft tissues influence the forces applied to the femur during falls. Yang and colleagues (2020) also investigated the relationship between fall orientation and hip fracture risk through an analysis of real-life fall videos. They found that hip fracture risk is associated with initial fall direction and landing configuration, with the highest risk during lateral and forward fall directions with sideways landing configurations. The orientation of the pelvis upon impact also influenced fracture risk, with most fractures occurring when the posterolateral aspect of the pelvis impacted the ground. In summary, hip fracture risk differs across fall direction and impact location. As will be illustrated in sections 2.2 and 2.3, soft tissues over the proximal femur influence impact forces during sideways falls and hip fracture risk. Accordingly, there is a need for comprehensive characterization of soft tissue thickness and composition over the proximal femur.

In addition to fall direction and impact orientation, the risk of hip fracture is also influenced by bone strength and soft tissue thickness. Previous research has found that hip fracture risk increases with decreased bone mineral density (BMD) (Johansson, Kanis, Odén, Johnell, & McCloskey, 2009; Kanis et al., 2005; Roberts et al., 2010), decreased soft tissue thickness (Bouxsein et al., 2007; Dufour et al., 2012; Dufour et al., 2019), and low body mass index (BMI) (De Laet et al., 2005; Johansson et al., 2014). It is important to note that BMI is highly correlated with trochanteric soft tissue thickness (TSTT) (Maitland, Myers, Hipp, Hayes, & Greenspan, 1993; Nielson et al., 2009; Schacter & Leslie, 2014). These results suggest that soft tissues have a protective effect during sideways falls onto the hip and may influence the amount of force that is transmitted from the skin surface to the femur

during an impact. Of importance to note, TSTT is only protective for low BMI females; TSTT is not protective for high BMI females or for males (Dufour et al., 2012; Nasiri & Luo, 2016). As will be shown in greater detail in sections 2.2 and 2.3, it is unclear how the differential components of soft tissues overlying the proximal femur may influence hip fracture risk. Overall, there is epidemiologic evidence which suggests that soft tissue properties over the proximal femur influence fracture risk. However, more research is needed to better understand the relationship between soft tissues, forces applied to the femur during a fall, and fracture risk.

Finally, sex is also a risk factor for hip fracture, with females having a greater risk of hip fracture than males (Chevalley, Guilley, Herrmann, Hoffmeyer, & Rizzoli, 2007). There are several factors behind this sex-based difference in hip fracture risk. First, females tend to have a lower bone mineral density (BMD) and begin to lose bone at a younger age and faster rate than males do (Alswat, 2017). This sex-based difference in BMD has direct impact on fracture risk as factors which alter the strength of the proximal femur affect its ability to withstand the loads applied during a fall. Second, the geometry of the female femur differs than that of males. Specifically, females have a lower femoral shaft cortex thickness, lower calcar femoral cortex width, lower femoral neck axis length, lower femoral head and femoral neck diameters, lower trochanteric width, and lower femoral shaft diameter than males do (Pulkkinen, Eckstein, Lochmüller, Kuhn, & Jämsä, 2006). These sex-based differences in femur geometry influence the strength of the proximal femur (Gregory & Aspden, 2008; Pulkkinen et al., 2006) and likely contribute to the higher hip fracture risk seen in females. Finally, body composition differs between males and females, with females having significantly less muscle, more adipose, and a larger proportion of their adipose tissues distributed over the hip and pelvis (Bredella, 2017; Ley, Lees, & Stevenson, 1992; Schorr et al., 2018). More relevant to the hip, females have significantly more soft tissues over the GT than males (Levine, Minty, & Laing, 2015). While previous research has investigated sex-based differences in general muscle thickness (Arts, Pillen, Schelhaas, Overeem, & Zwarts, 2010; Bredella, 2017; Hida et al., 2018; Schorr et al., 2018), general adipose thickness (Anvery et al., 2022; Bredella, 2017; Leahy, Toomey, McCreesh, O'Neill, & Jakeman, 2012; Schorr et al., 2018), and TSTT directly over the GT (Levine et al., 2015), there is a lack of research on sex-based differences in these individual tissues over the lateral proximal femur. Accordingly, understanding sex-based differences in the distribution of soft tissues overlying the proximal femur is crucial for better understanding the relationship between soft tissues and hip fracture risk.

2.2 Models of Hip Fracture

Hip fractures and hip fracture risk can be difficult to study in-vivo due to the traumatic nature of hip fracture; experimental studies are limited in what can be tested as the risk of injury to participants can be high. Cadaveric testing to investigate hip fracture and hip fracture risk is not limited by injury risk to participants, however results from cadaveric testing may not be directly applicable to in-vivo situations. Therefore, accurate models of hip fracture and hip fracture risk are crucial.

2.2.1 Cummings and Nevitt Conceptual Model of Hip Fractures

Fall-related hip fractures are multi-faceted events, with numerous factors playing a role in whether a fall-related fracture will occur. Cummings and Nevitt (1989) proposed a hypothesis on the cause of fall-related hip fractures. In their hypothesis, a series of four events must occur in order for a fall to result in hip fracture: 1) the faller must be oriented so that hip impact occurs; 2) the protective responses, such as extending the arms, must be insufficient to reduce the energy of the fall; 3) the local shock absorbers such as skin, muscle and adipose tissue must be insufficient in attenuating the impact energy; and 4) the strength of the proximal femur must be below the remaining energy of the fall. This hypothesis provides a systematic framework from which hip fractures can be examined and identifies several points where interventions and screening processes can be implemented. This thesis will focus on the third event in the Cummings and Nevitt (1989) hypothesis, which relates to the ability of local soft tissues to absorb and/or attenuate applied loads during the impact phase of a fall.

2.2.2 Biomechanical Models of Hip Fracture

The ability to accurately model fall-related hip fracture is important as in-vivo research on this subject is limited due to the risk of injury to human participants. From a biomechanical perspective, hip fractures can be examined using a factor of risk (FOR) approach, where hip fracture occurs when the forces applied to the proximal femur during a fall exceed the strength of the proximal femur (i.e. FOR > 1) (Dufour et al., 2012; Hayes et al., 1996). Therefore, hip fracture risk can be influenced by both the strength of the proximal femur and the force at which the hip impacts the ground. While both variables are important to consider when modelling hip fracture, this thesis will focus on factors influencing the loads applied to the femur and will only briefly touch on factors that influence bone strength.

Bone strength is one component of the FOR model of hip fractures and therefore, factors that influence the strength of the proximal femur will affect the likelihood of a fall-related hip fracture

7

occurring. A host of literature has explored the failure tolerance of the proximal femur. While numerous risk factors have been identified, the fracture forces range between 1997 to 5506 N. Table 1 presents a summary of studies in this domain. While I acknowledge the importance of tissue tolerance as a variable within the FOR model (and ultimately hip fracture risk), this thesis will focus on the applied load pathway.

Table 1: Results from studies reporting the strength (compressive force required to cause fracture) of the cadaveric proximal femur from older adults in a sideways fall loading configuration. Extracted from (Robinovitch et al., 2009).

Study	Condition	Mean(SD) fracture force (N)			Mean(SD or range) age in years, sample size		
		Women	Men	Mixed	Women	Men	Mixed
Lotz and Hayes, 1990[c]				2,110(1,060)			69(9); n=24
Courtney et al. 1994[c]	Deformation rate=100 mm/s			4,100(1,600)			74(7); n=8
	Deformation rate=2 mm/s			3,440(13,30)			74(7); n=8
Bouxsein et al. 1995[c]				3,680(1,540)			76(59-96)[b]; n=16
Pinilla et al. 1996[c]	0° Load angle			4050(900)			79(11); n=11
	15° Load angle			3,820(910)			81(7); n=11
	30° Load angle			3,060(890)			74(11); n=11
Cheng et al. 1997,1998[d]		3140(1240)	4630(1550)	3,980(1,600)	71(15); n=28	67(15); n=36	69(15); n=64
Bouxsein et al. 1999[c]		1997(1127)	3593(1614)	2,636(1,534)	82(13); n=16	78(10); n=10	81(12); n=26
Keyak et al. 2000[c]				2,400[a]			70(52-92)[a]; n=17
Lochmuller et al. 2002[d]		3,070(1060)	4,230(1530)		82(9); n=63	76(11); n=42	
Eckstein et al. 2004[d]				3,925(1,650)			79(11); n=54
Heini et al. 2004[c]				2,499(6,95)			76(7); n=20
Manske et al. 2006[c]				4,354(1,886)			69(16); n=23
Pulkkinen et al. 2006[d]		2,821[a]	4,209[a]	3,472[a]	82; n=77	79; n=63	81; n=140
Bouxsein et al. 2007[c]				3,353(1,809)			81(11); n=49
Pulkkinen et al. 2008[d]	Cervical fx	2,879(1,117)	4,079(1,165)		82(11); n=34	78(11); n=28	
	Trochanteric fx	3,053(976)	5,506(1374)				
Across study average		2,827	4,375	3,392	80	76	76

[a] SD not provided
[b] Range (not SD) reported
[c] Specimens were stored fresh-frozen
[d] Specimens were embalmed in alcohol/formalin
[e] Specimens were stored frozen, but the authors did not specify fresh versus embalmed.

Impact force is a key factor to consider when discussing hip fracture and hip fracture risk. Models for estimating impact force during sideways falls onto the hip are commonly used when studying fall induced hip fractures (Bouxsein et al., 2007; Dufour et al., 2012; Lafleur, Benoit R. et al., 2021; Martel, Daniel R. et al., 2020; Nielson et al., 2009; Roberts et al., 2010; Robinovitch, Hayes, & McMahon, 1991). Therefore, accurate predictions of impact force are imperative for accurate estimates of hip fracture risk. A mass-spring model is commonly used in the literature to predict

impact forces during lateral falls from standing height (Bouxsein et al., 2007; Dufour et al., 2012; Lafleur, Benoit R. et al., 2021; Martel, Daniel R. et al., 2020; Nielson et al., 2009; Roberts et al., 2010; Robinovitch et al., 1991). In this model, peak impact force is estimated based on the following equation:

$$Peak\ force = \sqrt{2ghmk}$$

Where g = gravitational constant, h = height of an individual's center of mass (0.51 * height), m = effective mass of the pelvis (total body mass * 0.467 for males, 0.553 for females in kg based on participants from Martel and colleagues (2018)*, k = stiffness constant (71 060 Nm for females, 90 440 Nm for males* (Robinovitch et al., 1991)*).*

However, **the above equation for predicting impact force during a sideways fall from standing height does not take into consideration any force attenuation by femoral soft tissues during a fall**. Femoral soft tissues, which are composed of the skin, subcutaneous adipose tissue, and muscle overlying the bony pelvis and femur, are known to affect the magnitude and distribution of forces at the skin surface and the underlying proximal femur during lateral falls onto the hip (Majumder, S. et al., 2013; Robinovitch et al., 1995). Using cadaveric tissues combined with a proximal femur impact pendulum, Robinovitch and colleagues (1995) determined that the force attenuation provided by trochanteric soft tissues during a sideways fall onto the hip is 71 N per 1 mm of soft tissue thickness. Therefore, the contributions of soft tissues to force attenuation during sideways falls can be accounted for in models of hip fracture by multiplying the TSTT (in mm) by 71. The predicted net impact force during a sideways fall can then be determined using the following equation:

$$Net\ impact\ force = peak\ force - (71 \times TSTT)$$

This approach is commonly used in the literature to account for force attenuation by trochanteric soft tissues during sideways falls onto the hip (Bachmann et al., 2014; Bhattacharya et al., 2019; Bouxsein et al., 2007; Dufour et al., 2012; Lafleur, Benoit R. et al., 2021; Martel, Daniel R. et al., 2020; Nielson et al., 2009; Roberts et al., 2010). While this approach is commonly used, it is associated with several *limitations*:

1) They tested cadaveric tissues.

2) They had a small sample size of only 9 specimens.

9

3) They tested a small range of soft tissue thickness (thickness ranged from 8 – 43 mm, with an average thickness of 24 ± 13 mm).

4) They considered the soft tissues as one bulk tissue, without considering the contribution of muscle and adipose tissue to the total thickness.

5) They only considered the soft tissues lying directly over the GT.

The _implications_ of these limitations are as follows:

1) The response of cadaveric tissues may be different than the response of in-vivo tissues.

2) The small sample size reduces our ability to generalize the results of this study to a larger population.

3) Due to the small range of tissue thicknesses that were tested, the force attenuation relationship for soft tissues may not be applicable to individuals with larger amounts of TSTT.

4) Muscle and adipose tissues have different mechanical properties. Therefore, these individual tissues may differentially contribute to the forces attenuated by the bulk TSTT.

5) There is no consideration for potential changes in the force attenuating capabilities of the proximal femur soft tissues at locations other than those directly over the GT.

This thesis aims to address these limitations in current methods for accounting for force attenuation by trochanteric soft tissues by considering the contribution of muscle and subcutaneous adipose tissue to bulk soft tissue thickness over multiple locations on the lateral proximal femur. Additionally, measures used to inform fracture risk should be reliable. Therefore, this thesis will explore the reliability of individual tissue thickness measures.

2.2.3 Finite Element (FE) Models of Hip Fracture

FE models of the hip recognize the importance of incorporating femoral soft tissues, however, there is variance in the geometry used in these models and a lack of incorporation of individual soft tissues across studies. Table 2 presents a summary of FE models of the hip that have been used for studying hip fracture. While these models incorporate soft tissues, they only consider a singular material (i.e. don't differentiate muscle from adipose). Additionally, in some cases the variance in soft tissue thickness over different regions of the proximal femur is either not incorporated (Nasiri & Luo, 2016;

Sarvi & Luo, 2015), not specified (Fleps et al., 2018; Fleps et al., 2019; Galliker et al., 2022; Majumder, S. et al., 2008; Majumder, S. et al., 2013; Majumder, Santanu et al., 2007; Nasiri & Luo, 2016; Sarvi & Luo, 2015), or is derived from a relatively small number of participants (< 10) (Fleps et al., 2018; Fleps et al., 2019; Galliker et al., 2022; Majumder, S. et al., 2008; Majumder, S. et al., 2013; Majumder, Santanu et al., 2007; Nasiri & Luo, 2016; Sarvi & Luo, 2015). Accordingly, there is a critical need for experimental studies with human participants to provide more biofidelic inputs (including thickness of individual soft tissues over a greater number of locations on the proximal femur) to FE models. Doing so will support improved outputs from computational models and increase our ability to design effective hip fracture intervention techniques based on outputs from computational models. Section 2.2.5 provides details on the influence of soft tissues on these interventions.

Table 2: Table describing finite element models of the hip

Author/Year	Methods	FE Model Skin Surface Geometry	Soft Tissues Modeled	Soft Tissue Thickness	Limitations
Majumder et al. (2007)	Nonlinear FE model of human pelvis-femur-soft tissue complex	Surface geometry to match a 58-year-old male	Ligaments, bulk TSTT (no separation of muscle and adipose)	14 mm over GT	Only a bulk soft tissue modelled. Only a single person modelled.
Majumder et al. (2008)	Nonlinear FE model of human pelvis-femur-soft tissue complex developed by Majumder et al. (2007)	Surface geometry to match a 58-year-old male	Ligaments, bulk TSTT (no separation of muscle and adipose)	5 mm, 14 mm, 17 mm, 23 mm, and 26 mm All soft tissue thickness measurements are over the GT	Soft tissue thickness is assumed to be the same over the entire surface contacting the ground Only a bulk soft tissue modeled. Only a single person modeled.
Majumder et al. (2013)	FE models of 7 male human pelvis-femur-	Subject-specific surface geometry with constant	Ligaments, bulk TSTT (no separation of	5 mm, 14 mm, 17 mm,	Soft tissue thickness is assumed to

	soft tissue complexes	underlying bone geometry and properties to match a 58 year old male	muscle and adipose)	23 mm, and 26 mm All soft tissue thickness measurements are over the GT	be the same over the entire surface contacting the ground Only a bulk soft tissue modeled. Only a single person modeled.
Sarvi & Luo (2015)	Whole body dynamics model and FE model of the proximal femur	N/A. No soft tissues incorporated into FE model.	Bulk TSTT	Low BMI: 24.3 (10.2) mm Normal BMI: 44.7 (16.6) mm Overweight: 55.5 (11.9) mm Obese: 73.4 (25.3) mm	Only considered bulk soft tissue thickness Soft tissues weren't directly modelled in the FE model. They were included in the dynamics model instead.
Nasiri & Luo (2016)	Whole body dynamic model and FE model of the proximal femur	N/A. No soft tissues incorporated into FE model.	Bulk TSTT	Male average TSTT: 49.9 (23.1) mm Female average TSTT: 54.3 (23.3) mm	Only considered bulk soft tissue thickness Soft tissues weren't directly modelled in the FE model. They were included in the dynamics model instead.

Fleps et al. (2018)	Dynamic linear and non-linear and FE model constructed from CT scan data	Soft tissue geometry to match subjects in an existing body shape database (one male and one female)	Cartilage, ligaments, bulk TSTT	Male: 31 mm Female: 32 mm	TSTT modelled as a bulk tissue and modelled based on experimental data that used ballistics gel as a soft tissue surrogate 2 specimens with similar TSTT modelled
Fleps et al. (2019)	Subject specific FE models of 6 females and 5 males aged 54 – 94 (average age 77.1 (13.4) years	Soft tissue geometry to match subjects tested in experimental study by Fleps et al. (2018)	Cartilage, ligaments, bulk TSTT	Range: 7 – 76 mm Average: 22.7 (7.8) mm	Bulk TSTT modelled (no consideration of muscle and adipose) based on experimental data using ballistics gel as a soft tissue surrogate
Galliker et al. (2022)	FE model of a generic hip protector combined with a subject-specific FE model of 2 males and 2 females	Hip protector FE model created using surface geometry of a low BMI female (BMI = 15.4 kg/m^2) Soft tissue geometry in subject-specific FE model to match subjects tested in Fleps et al. (2018) and Fleps et al. (2019).	Cartilage, ligaments, bulk TSTT	10 mm, 14 mm, 19 mm, 76 mm	Bulk TSTT modelled (no consideration of muscle and adipose) based on experimental data using ballistics gel as a soft tissue surrogate

2.2.4 Force Distribution during an Impact

In addition to load magnitude, soft tissues in the hip region influence impact dynamics factors including the point of application and direction of impact force. Table 3 provides a description of recent work in this area. In summary, work done by Pretty et al. (2021b; 2021a) has shown that contrary to previous research showing that peak impact forces are applied directly to the GT during a sideways fall (Cummings & Nevitt, 1989; Robinovitch et al., 1991), peak pressure is located distally and posteriorly to the GT. This has significant implications for research into hip fractures and hip fracture intervention techniques, however, there are two major limitations with this work that are of direct relevance to this thesis: 1) The authors only considered bulk soft tissue thickness; and 2) the authors only considered the soft tissues lying directly over the GT. Related to the first limitation, the mechanical properties of muscle and adipose tissue are different, therefore their ability to absorb and distribute loads will be different. Accordingly, it is important to consider the thickness of the individual soft tissues when investigating their relationship to force distribution during a fall. Regarding the second limitation, the thickness and composition of the soft tissues may change at different locations over the femur. Accordingly, only considering soft tissue thickness directly over the GT may not provide the most accurate picture of how the soft tissues respond during an impact. More in-depth characterization of the soft tissues overlying the proximal femur are needed as they could provide enhanced insights into the relationship between femoral soft tissues and force distribution during an impact. This thesis will contribute to the body of literature focused on understanding the role of soft tissues during an impact by providing a more in-depth characterization of the soft tissues. Specifically, by characterizing the thickness and distribution of the individual soft tissues overlying multiple locations on the lateral proximal femur.

Table 3: Table describing studies on pressure distribution during sideways falls

Author/Year	Objectives	Methods	Soft Tissue Thickness (mm)	Location of Peak Impact Force/Peak Pressure
Pretty et al. (2021a)	Investigate the influence of fall simulation paradigm (FSP), sex, and TSTT on pressure distribution during sideways falls onto the hip	FSP 21 females 19 males	Females: -low: 30 (4) mm -mid: 42 (3) mm -high: 66 (17) mm Males: -low: 24 (4) mm -mid: 35 (3) mm -high: 49 (11) mm	Peak pressure located distal and posterior to the GT in all FSP, TSTT, and sex groups Greater force localization over the GT in pelvis release, males, and low TSTT groups
Pretty et al. (2021b)	To investigate the influence of sex and TSTT on peak impact vector magnitude, orientation, and center of pressure during simulated falls	FSP 21 females, 19 males aged <35 years	Females: -low: 30 (4) mm -mid: 42 (3) mm -high: 66 (17) mm Males: -low: 24 (4) mm -mid: 35 (3) mm -high: 49 (11) mm	Sex and TSTT influence force magnitude and center of pressure with lower force and more distal force application in females and high TSTT participants. Peak pressure located on average distal and posterior to the GT

2.2.5 Effects of Soft Tissues on Hip Fracture Impact Attenuation Interventions

As previously demonstrated, the soft tissues overlying the proximal femur play a critical role in influencing impact forces during a sideways fall onto the hip. In addition to this, soft tissues also influence the effectiveness of hip fracture intervention techniques (Bhan, Levine, & Laing, 2013; Galliker et al., 2022; Laing & Robinovitch, 2008; van Schoor, Van der Veen, Schaap, Smit, & Lips, 2006). Two common hip fracture prevention techniques are wearable hip protectors and compliant (i.e. safety) floors. These interventions are designed to absorb and dissipate energy during an impact, which reduces the risk of a fall-related hip fracture (Bhan et al., 2013; Galliker et al., 2022; Laing & Robinovitch, 2008; van Schoor et al., 2006). Hip protectors and compliant floors are discussed in more detail below, including the role that soft tissues play in the effectiveness of these interventions.

2.2.5.1 Hip Protectors

Wearable hip protectors, which are undergarments with either a hard or a soft shell covering the user's proximal femur, are one intervention that can be used to mitigate the risk of a fall-related hip fracture. They have been shown to attenuate impact forces during sideways falls (Galliker et al.,

2022; Laing & Robinovitch, 2008; van Schoor et al., 2006) and reduce the risk of fall-related hip fractures when worn at the time of a fall (Korall et al., 2019). However, the amount of force attenuation provided by hip protectors is dependent upon thickness of the underlying soft tissues (Galliker et al., 2022; Laing & Robinovitch, 2008; van Schoor et al., 2006).

Using a mechanical test system, van Schoor and colleagues (2006) found that the force attenuating capabilities of hard-shell hip protectors were similar between tests with 0.5 inches of soft tissues and 1 inch of soft tissues (67 – 86% and 68 – 80% respectively). However, the efficacy of soft-shell hip protectors was heavily influenced by soft tissue thickness. As soft tissue thickness increased from 0.5 inches to 1 inch, the force attenuation provided by different models of hip protectors changed by 25-56%. Building upon this work, Laing and colleagues (2008) explored the influence of soft-shell hip protectors on pressure distribution during pelvis release experiments with human volunteers. Once again, the efficacy of hip protectors was dependent upon soft tissue thickness. They found that as BMI, which is highly correlated with TSTT (Maitland et al., 1993; Nielson et al., 2009; Schacter & Leslie, 2014), decreased, the force attenuation provided by hip protectors increased. Finally, Galliker and colleagues (2022) used an FE model to investigate the influence of hip protectors on hip fracture risk. Similar to Laing and colleagues (2008), Galliker et al. (2022) found that hip protectors provided greater force attenuation in low BMI/low TSTT subjects compared to high BMI/high TSTT subjects. Taken together, the results from these studies highlight the influence of soft tissues on the efficacy of hip protectors. Accordingly, an improved understanding of soft tissue composition and distribution is crucial to improving the design of hip protectors.

2.2.5.2 Compliant Floors

Compliant (i.e. safety) floors are another hip fracture intervention technique that uses impact attenuation to reduce the risk of fall-related hip fractures. This type of flooring has been shown to attenuate impact forces during sideways falls onto the hip (Laing & Robinovitch, 2009). Similar to hip protectors, the ability for compliant floors to absorb energy during an impact is influenced by soft tissues. Bhan and colleagues (2013) used a pelvis release experimental paradigm with human volunteers to investigate the influence of BMI on the force attenuation provided by compliant floors during simulated lateral falls. Results from this study show that there is a significant influence of BMI on force attenuation provided by compliant floors, with compliant floors attenuating 18.4% of impact forces in the low BMI group and 0.3% of impact forces in the high BMI group. Accordingly, understanding the composition and distribution of soft tissues over the proximal femur is crucial to

understanding the mechanisms behind the differences in force attenuation provided by compliant floors between high and low BMI individuals, and improving the efficacy of this prevention technique for everyone.

2.3 Existing Measures of TSTT

Several imaging modalities have been used to characterize soft tissue thickness over the GT.

Table 4 provides a comprehensive description of all the relevant literature. To further discuss this literature, it has been categorized by imaging modality, with limitations and gaps in the literature discussed at the end of this section.

Eight studies have used ultrasound to measure TSTT (Choi, Russell, Tsai, Arzanpour, & Robinovitch, 2015; Lafleur, Benoit, 2016; Lafleur, Benoit R. et al., 2021; Levine et al., 2015; Lim & Choi, 2021; Maitland et al., 1993; Minns, Marsh, Chuck, & Todd, 2007; Robinovitch et al., 1991). The mean TSTT values in these studies range from 11.4 to 55.7 mm. Seven studies have used Dual Energy X-Ray Absorptiometry (DXA) or Computed Tomography (CT) to measure TSTT (Bouxsein et al., 2007; Etheridge et al., 2005; Lafleur, Benoit, 2016; Maitland et al., 1993; Nielson et al., 2009; Schacter & Leslie, 2014; Town et al., 2022). The mean TSTT values in these studies range from 29.1 to 49.8 mm. Only one study has directly measured TSTT using pins(Robinovitch et al., 1995). The TSTT values in this study range from 8 to 45 mm, with a mean value of 24 ± 13 mm.

Across the range of studies measuring TSTT, there are two gaps in the literature that are consistent across all the studies. The first gap is that soft tissue thickness is measured as one bulk tissue thickness. There is no consideration for the thickness of the individual soft tissues (i.e. muscle thickness and adipose thickness). The second gap is that the studies focus on measuring TSTT, with little consideration for the thickness of the soft tissues at other locations over the proximal femur. These are important gaps to address as muscle and adipose tissue have different mechanical properties, and therefore accounting for their individual thicknesses is crucial for improving hip fracture models and intervention techniques. Additionally, Pretty et al. (2021b; 2021a) showed that peak pressure during a sideways fall is located distal and posterior to the GT, therefore focusing on soft tissue thickness directly over the GT may not provide the most accurate picture of how soft tissues influence impact forces and fracture risk during sideways falls. This thesis aims to address

these critical gaps in the literature by characterizing the thickness of muscle and adipose tissue over multiple locations on the proximal femur.

Table 4: Table describing studies that have measured or estimated TSTT

Authors/Year	Category	Sample Size	Age (years)	Soft Tissue Thickness (mm)	Method	Major Findings
Robinovitch et al. (1991)	Role of soft tissues during an impact	7 males 7 females	Mean: 26.9 ± 5.5 Range: 20 – 35	Mean: 26.1 ± 12.7 Range: 9 – 50	Ultrasound while standing	TSTT influences stiffness of the pelvis with increased TSTT reducing stiffness and subsequent impact forces
Robinovitch et al. (1995)		3 males 6 females (cadavers)	Mean: 72 ± 4 Range: 60 - 102	Mean: 24 ± 13 Range: 8 – 45	Direct measurement using pins	1 mm of TSTT attenuates 71 N of force during simulated sideways falls
Etheridge et al. (2005)		10 female pelvises	Mean: 75.9 ± 8.6 Range: 53 – 82	Mean: 41.3 ± 18.8 Range: 13.4 – 79	CT	Energy dissipated by TSTT changes with impact velocity
Choi et al. (2015)		17 young adult females 17 older adult females	Mean: 21.2 ± 2.7 Mean: 69.9 ± 4.7	Mean: 32.1 ± 7.2 Mean: 30.4 ± 14.9	Ultrasound while side-lying	No differences in TSTT, muscle thickness, fat thickness or skin thickness between older and younger women. This is the only study that measured muscle and adipose thickness. Stiffness and damping is greater in young compared to

						older women, however neither correlated with soft tissue thickness
Lim and Choi (2021)		9 males 9 females	Range: 19 – 27	Measured but not reported	Ultrasound	Energy absorption by soft tissues ranged from 0.03 – 3.05 J. Energy absorption depended on impact configuration (62% more in posterolateral than anterolateral) No sex-based differences in energy absorption.
Bouxsein et al. (2007)	TSTT and Fracture Risk	42 female controls 21 female fracture cases	Mean: 73.9 ± 8 Mean: 73.9 ± 8.3	Mean: 49.8 ± 16.8 Mean: 40.4 ± 16.7	Whole body DXA	TSTT significantly different between fracture cases and controls. TSTT trended towards being a predictor of hip fracture, independent of BMD.
Nielson et al. (2009)		222 male controls 70 male fracture cases	Mean: 74.2 ± 6.1 Mean: 79.7 ± 6	Mean: 31 ± 11.5 Mean: 29.1 ± 11.9 Range: 13.3 – 78	Whole body DXA and subset of QCT	TSTT not significantly different between fracture cases and controls, however FOR was.
Roberts et al. (2010)		48 females 25 males (cadavers)	Mean: 74.38 ± 8.91	Mean: 41.86 ± 30.84	BMI regression equations	FOR was a better predictor of hip fracture

Study	Category	Sample	Age	Value	Method	Findings
			Range: 55 – 98			than BMD T-scores alone
Dufour et al. (2012)		425 males (26 fractures)\n\n675 females (110 fractures)	Mean: 76 ± 5.1\n\nRange: 67 – 95	30.1 ± 9.3\n29.5 ± 9.9\n\n55.3 ± 16.8\n49.5 ±16.8	BMI regression equations	FOR significantly associated with hip fracture in men and women.\n\nFall force and TSTT predictive of hip fracture, independent of BMD, in women but not in men.
Maitland et al. (1993)	Measurement Technique	50 females	72 ± 4	15 – 85	Ultrasound while standing and DXA	Significant correlation between ultrasound measured TSTT, DXA, BMI, BIA, and hip circumference
Minns et al. (2007)		12 female controls\n\n20 female fracture cases	69 – 88\n\n76 – 93	27.9\n\n18.1	Ultrasound while standing	Showed GT is 12 cm posterolateral from the ASIS and provided insights for how hip protectors should be positioned
Schacter and Leslie (2014)		376 adults randomly split into 2 cohorts	56.6 ± 20.8\n\n54.8 ± 20.1	49 ± 23\n\n48 ± 21\n\n3 – 140	Whole body DXA	Predicted TSTT based on sex, BMI, average spine thickness, and average hip thickness
Levine et al. (2015)		10 females\n\n10 males	22.3 ± 1.1\n\n22.2 ± 1.9	33.3 ± 6.6\n\n22.8 ± 9.7\n\nAll: 28.1 ± 9.7	Ultrasound while standing	Postural changes (flexion, extension, flexion + adduction) and sex (male,

						female) influence TSTT
Lafleur (2016)		25 females 20 males 45 total	68.5 ± 11.9 72.5 ± 9.1 70.2 ± 10.8	Mean ultrasound measured TSTT: -Side-lying: 32.9 ± 17 -Standing: 41.6 ± 21 -Supine: 55.7 ± 28 -Range: 11.4 – 122.1 Mean DXA measured TSTT: 47.5 ± 23 -Range: 11 – 105	Ultrasound while standing, side-lying, and supine with 25 degrees internal hip rotation, no hip rotation, and 25 degrees external hip rotation Whole body DXA	TSTT significantly different between standing, supine, and side-lying measurements (exceeded the clinically relevant difference of 0.96 cm). Differences in TSTT across hip rotations did not reach the clinically relevant difference. Concordance validity between supine ultrasound and DXA is poor.
Town et al. (2022)		DXA: young adults (13 males, 13 females) & older adults (13 males, 12 females) Predictive equations: DXA: young adults (37 males, 37 females) & older adults (38 males, 38 females)	Young adults: 16 – 35 Older adults 36 – 65	DXA TSTT: 38.1 – 47.5 Predicted TSTT: 35.3 – 46.3 DXA iliac crest thickness: 21.4 – 39.5 Predicted iliac crest thickness: 23.6 – 38.4	Whole body DXA Predictive equations	Soft tissue thickness over the GT and iliac crest can be accurately predicted from equations using anthropometric measurements. This is the only study that measured soft tissue thickness at a location other than the GT

Lafleur et al. (2021)	Combined fracture risk and measurement technique	25 females 20 males 45 total	68.5 ± 11.9 72.5 ± 9.1 70.2 ± 10.8	Side-lying mean: 32.9 ± 17 Standing mean: 41.6 ± 21 Supine mean: 55.7 ± 28 Range: 11.4 – 122.1	Ultrasound while standing, side-lying, and supine with 25 degrees internal hip rotation, no hip rotation, and 25 degrees external hip rotation	TSTT significantly different between standing, supine, and side-lying measurements (exceeded the clinically relevant difference of 0.96 cm). Differences in TSTT across hip rotations did not reach the clinically relevant difference. Predicted impact forces and FOR significantly influenced by body position and hip rotation.

2.4 Imaging Modalities: Ultrasound vs. DXA

As demonstrated in section 2.3, ultrasound and DXA are the two most common methods for measuring TSTT. This section will provide a description of how these two imaging modalities work and a discussion about the benefits and limitations of each to highlight the rationale for selecting ultrasound as the imaging modality used in this thesis.

2.4.1 Ultrasound

Ultrasound devices generate soundwaves between 1 – 20 MHz by turning electrical energy into mechanical energy. The ultrasound transducer (a.k.a. the ultrasound probe) contains piezoelectric crystals that vibrate as an electrical signal is applied to the transducer. As the piezoelectric crystals vibrate, they produce high frequency ultrasound waves which are transmitted into the body (Chan & Perlas, 2011). As they encounter tissues in the body, some of the ultrasound waves are reflected back to the transducer while some continue to penetrate deeper into the body. The velocity and intensity of

the returning echo is dependent upon the tissue the ultrasound wave encountered (Chan & Perlas, 2011; Kossoff, 2000). As the reflected ultrasound waves travel back to the transducer, they cause the piezoelectric crystals to vibrate and deform, converting the ultrasound waves back into electrical signals. The computer turns the returned signal into points of brightness on the image based on the velocity of the ultrasound waves and the intensity of the echo (Chan & Perlas, 2011).

There are several types of ultrasound transducers: linear array, phased array, annular array, and single element disc transducers (Kossoff, 2000). In studies involving ultrasound measured TSTT, either linear or curvilinear array probes are most commonly used (Choi et al., 2015; Lafleur, Benoit, 2016; Lafleur, Benoit R. et al., 2021; Levine et al., 2015; Lim & Choi, 2021; Maitland et al., 1993; Minns et al., 2007; Robinovitch et al., 1991), therefore the remainder of the discussion on ultrasound probes will be focused on these two types of probes. Linear array probes have a rectangular field of view and generate ultrasound waves in straight lines while curvilinear array probes have a cone-like field of view and generate sound waves in a cone-like pattern (beam is narrower by the probe and gets wider as it travels away from the probe). Compared to linear array probes, curvilinear probes cover a wider field of view and have greater penetration depth, however this increased penetration depth comes at the expense of reduced image resolution (Chan & Perlas, 2011; Markowitz, 2011). In contrast, the linear array probe has a better image resolution, however this comes at the expense of penetration depth. It is not capable of imaging the same depths as a curvilinear probe, and as imaging depth increases, the field of view becomes smaller (Chan & Perlas, 2011; Markowitz, 2011). The difference in penetration depth between the two types of probes is due to the different frequencies they operate at: curvilinear probes tend to operate at lower frequencies while linear probes tend to operate at higher frequencies. Lower frequency probes can penetrate deeper into the body due to lower attenuation of the sound waves as they travel through the tissues when compared to higher frequency probes (Chan & Perlas, 2011; Markowitz, 2011). As will be explained in greater detail in sections 2.5, 2.6, **Error! Reference source not found.**, and 3.1, this thesis aims to differentiate between muscle and adipose tissue, and measure the thickness of these individual tissues. Therefore, a linear probe will be used during data collection to ensure high resolution images are obtained.

There are several benefits to using ultrasound over other imaging modalities: 1) ultrasound is a non-invasive modality for imaging soft tissues; 2) does not expose participants to harmful radiation; 3) is relatively simple to use; 4) correlates well with other subcutaneous soft tissue measurement techniques (Black, Vora, Hayward, & Marks, 1988; Hansen & Kehrer, 1987; Maitland et al., 1993);

5) is clinically accessible and relatively portable; 6) can be used to measure thickness over a large range of body parts; and 7) has been shown to be a reliable method for measuring soft tissue thickness (Betz, Wehrstein, Preisner, Bendszus, & Friedmann-Bette, 2021; Black et al., 1988; Lafleur, Benoit, 2016; Lanza, Rock, Marchese, Gray, & Addison, 2022; Levine et al., 2015; Mendis, Wilson, Stanton, & Hides, 2010; Thoirs, Kerry & English, 2009). While several studies have previously investigated the reliability of ultrasound measured soft tissue thicknesses throughout the body (Betz et al., 2021; Black et al., 1988; Lafleur, Benoit, 2016; Lanza et al., 2022; Levine et al., 2015; Mendis et al., 2010; Thoirs, Kerry & English, 2009), there has been no investigation of the reliability of ultrasound measured muscle, adipose, and total soft tissue thickness over the lateral proximal femur in a simulated sideways fall configuration. Having a reliable method for measuring tissue thicknesses in this region is crucial to improving our understanding of the role of soft tissues during sideways falls onto the hip. This thesis aims to address this gap in the literature by investigating the intra-rater reliability of ultrasound measured tissue-specific thicknesses over the lateral proximal femur.

There are limitations with the use of ultrasound that are worth discussing: 1) even though it is relatively simple to use, proper technique and knowledge of how to obtain high quality images is imperative to getting good results when using ultrasound to measure soft tissue thickness; and 2) obtaining high quality images with clear differentiation between tissues types on participants with larger amounts of soft tissue thickness can be difficult because as penetration depth increases, image resolution decreases (Markowitz, 2011).

2.4.2 DXA

DXA scans are commonly used to measure bone mineral density, however they can also be used to measure lean mass, fat mass, and bulk tissue thickness (Lafleur, Benoit, 2016; Laskey, 1996; Maitland et al., 1993; Nielson et al., 2009; Town et al., 2022). A DXA scanner consists of an x-ray generator, a detector, and a computer system. During a scan, x-rays of two different energies are generated and passed through the participant. As the x-ray beams pass through the body, they are differentially attenuated as they pass through bone and soft tissues. The detector reads the energy that has passed through the body and determines the level of x-ray attenuation. The computer then generates an image based on how much energy is attenuated by bone and soft tissues (Berger, 2002; Laskey, 1996). Post hoc analysis is required to obtain values for lean mass, muscle mass, and bone mineral density (Laskey, 1996). Post hoc analysis is also required to obtain measurements of soft tissue thickness (Lafleur, Benoit, 2016; Nielson et al., 2009).

Similar to ultrasound, DXA has been shown to be a reliable method for measuring soft tissue thickness, with excellent intra and inter-rater reliability (Lafleur, Benoit, 2016; Schacter & Leslie, 2014; Town et al., 2022). Other benefits of using DXA include: 1) a DXA scan is relatively quick; 2) soft tissue thickness measurements can be obtained on patients who are already getting a bone mineral density scan; 3) the scan is done in a supine position, which may be a more comfortable position for participants than some ultrasound studies; and 4) it doesn't require exposing the hip for imaging, which may also improve participant comfort levels. However, there are several limitations associated with the use of DXA for measuring soft tissue thickness: 1) it exposes participants to harmful radiation; 2) it is not portable; 3) participants are supine, which may alter thickness measurements (Bouxsein et al., 2007); 4) soft tissue thickness cannot be measured in real-time, and post-hoc analysis of the image can be time consuming (Nielson et al., 2009); 5) thickness measurements are limited to those that can be measured in the same plane as the DXA scan (i.e. on the lateral and medial aspects of the body); and 6) DXA cannot provide the thickness of individual soft tissues (muscle and adipose tissue). Because of these limitations, and the goals of this thesis, ultrasound was chosen as the imaging modality for use in data collection.

2.5 Key Gaps in the Literature

This project aims to address the following key gaps in the literature:

1. Previous research on the relationship between soft tissues and hip fracture has only considered bulk soft tissue thickness, without consideration of the differing contributions of muscle and subcutaneous adipose tissue to total thickness. Considering the contributions of the individual soft tissues when studying the relationship between soft tissues and hip fracture is important as the tissues may differentially contribute to energy absorption, and therefore fracture risk, during a sideways fall. This thesis aims to address this gap by measuring the individual thickness of muscle and subcutaneous adipose tissues.

2. Previous research on the relationship between soft tissues and hip fracture has focused on the soft tissues directly overlying the GT, despite evidence that the principle impact sites during a sideways falls are distal to the GT. To further our understanding of the role of soft tissues in hip fracture, it is necessary to study the soft tissues surrounding the GT. This thesis aims to address this gap by examining soft tissue thickness and composition from multiple locations around the proximal femur.

3. Previous research on the relationship between soft tissues and hip fracture has measured soft tissue thickness in standing, supine, and side-lying positions, however, there has been no measurement of soft tissue thickness in a simulated sideways fall configuration. To further our understanding of the role of soft tissues in hip fracture, it is necessary to study the soft tissues in a relevant fall orientation. This thesis aims to address this gap in the literature by examining the soft tissues in a simulated sideways fall configuration, where tissues are measured from the side of the body that would impact the ground during a fall event.

2.6 Thesis Objectives and Hypotheses

This thesis has two main objectives:

1. To assess the reliability of a novel ultrasound protocol for characterizing soft tissue thickness and composition from multiple locations around the lateral proximal femur.

2. To assess location and sex-specific soft tissue thickness and composition from multiple locations around the lateral proximal femur.

My primary interests were related to assessing location and sex-based differences in soft tissue thickness and composition (objective 2), however, to have confidence in the measures taken to explore these differences, the reliability objective (objective 1) was also addressed.

Specifically, objective 1 of this thesis aims to answer the following questions:

1a. What is the intra-rater reliability of ultrasound thickness measurements at 12 measurement locations over the proximal femur for measurements of total soft tissue thickness (TST), muscle thickness (MT), and subcutaneous adipose tissue thickness (AT)?

1b. Does intra-rater reliability differ between locations over the proximal femur (12 locations) for TST, MT, and AT?

Objective 2 of this thesis aims to answer the following question:

2. Are there differences in TST, MT, or AT based on sex (male, female) and measurement location?

It is hypothesized that:

26

1. The intra-rater reliability of all soft tissue thickness measurements will be good to excellent (ICC > 0.75).
2. Intra-rater reliability will differ between locations over the proximal femur, with reliability being lower for measurements on the anterolateral and posterolateral femur compared to the lateral femur.
3. There will be a main effect of sex on all soft tissue thickness measurements. It is expected that:
    3a. TST will be greater in females than males.
    3b. MT will be greater in males than females.
    3c. AT will be greater in females than males.
4. There will be a main effect of measurement location on all soft tissue thickness measurements. It is expected that:
    4a. TST will be greater over the posterolateral femur compared to the lateral or anterolateral femur.
    4b. MT will be greater over the posterolateral and anterolateral femur compared to the lateral femur. Compared to all other locations, MT will be lowest directly over the GT.
    4c. AT will be greatest over the posterolateral femur and lowest over the anterolateral femur.

Chapter 3
Research Experiment

3.1 Methods

3.1.1 Participants

25 participants (12 males and 13 females) aged 18 – 35 years old with self-reported BMI $\leq$ 24.9 kg/m^2 were recruited for this study.

3.1.1.1 Inclusion/Exclusion Criteria

Participants were excluded from this study if they:

      1. Were not between the ages of 18 – 35 years.

      2. Had a self-reported BMI > 24.9 kg/m^2.

      3. Had a recent or chronic hip or pelvic injury, including hip replacement.

      4. Had bariatric surgery or gained or lost 25 or more pounds in the last year.

      5. Had a recent injection of a gaseous contrast media to the hip or pelvic area.

      6. Were pregnant or suspected they may be.

      7. Had a known allergy to ultrasound gel, rubbing alcohol, tapes, or adhesives.

The rationale for excluding high BMI individuals is that this thesis aims to measure MT and AT as well as TST. In order to do so, high quality ultrasound images are needed to clearly differentiate between the different tissue types. A linear ultrasound probe provides higher quality ultrasound images with improved image resolution compared to a curvilinear probe (Figure 3-1; (Markowitz, 2011)). However, the improved image quality with a linear probe comes at the expense of penetration depth (14 cm for the linear probe compared to 30 cm for the curvilinear probe). Collecting only low and normal BMI individuals will ensure that high quality images can be captured, allowing for clear differentiation between MT and AT, without exceeding the probe's depth capabilities. Additionally, high BMI individuals are at a lower risk of hip fracture compared to low BMI individuals (De Laet et al., 2005; Johansson et al., 2014). Therefore, it is most important to capture individuals of low and normal BMI in the data set.

28

Figure 3-1: Comparison of ultrasound images taken with the linear probe and curvilinear probe taken at measurement location A3. The image quality is improved with the linear probe, allowing for easier differentiation between muscle and adipose tissue. Additionally, the surface of the skin is easier to identify with the linear probe compared to the curvilinear probe.

3.1.2 Recruitment

Participants were recruited from the University of Waterloo using recruitment posters placed around campus and email recruitment scripts. All experimental procedures were approved by the Office of Research Ethics at the University of Waterloo (ORE #41814).

3.1.3 Instrumentation

A GE LOGIQ E10 commercial ultrasound machine (Figure 3-2; GE Healthcare Canada, ON, Canada) and a L2-9VN-D linear array ultrasound probe (Figure 3-2; GE Healthcare Canada, ON, Canada) with a frequency bandwidth of 2 – 9 MHz was used to obtain ultrasound images at 12 locations over the proximal femur (more details below on measurement locations). Ultrasound was chosen as the method for imaging the soft tissues over the hip and femur as it is an accessible, non-invasive modality for imaging soft tissues that does not expose participants to harmful radiation, correlates well with other subcutaneous soft tissue measurement techniques (Black et al., 1988; Hansen & Kehrer, 1987; Maitland et al., 1993), and has been previously employed in the literature (Choi et al., 2015; Hansen & Kehrer, 1987; Lafleur, Benoit, 2016; Lafleur, Benoit R. et al., 2021; Levine et al., 2015; Lim & Choi, 2021; Maitland et al., 1993). The rationale for selecting a linear array ultrasound probe instead of a curvilinear probe is that this thesis aims to differentiate between muscle and adipose tissue. To do so, high quality ultrasound images are needed to clearly differentiate between

29

the different tissue types. A linear ultrasound probe provides higher quality ultrasound images with improved image resolution compared to a curvilinear probe (Figure 3-1; (Markowitz, 2011)). While the linear array probe produces images with better resolution, this image resolution comes at the expense of penetration depth. The linear probe is only capable of imaging structures up to 14 cm of depth (in the general MSK setting) and as penetration depth increases, the field of view becomes narrower. Accordingly, the linear probe may not be appropriate for measuring soft tissue thickness in high BMI individuals.

For all images, a general musculoskeletal imaging setting (MSK Gen) was used. Image depth and gains were adjusted as needed to obtain the best quality image at each measurement location and for each individual participant.

Collected ultrasound images were analyzed using the ultrasound machine's built-in measurement software to determine TST, MT, and AT as described in detail in the Data Analysis section below.

https://www.gehealthcare.com/products/ultrasound/logiq/logiq-e10   https://theultrasoundsource.com/ge-l2-9vn-d-linear-probe/

Figure 3-2: GE LOGIQ E10 ultrasound machine (left) and L2-9VN-D linear array ultrasound probe (right)

3.1.4 Experimental Protocol

Verbal and written informed consent were obtained from all participants. Participants were asked to change into loose-fitting shorts and a comfortable t-shirt. Following this, participant height and weight were measured for BMI calculations.

To simulate a lateral fall configuration, participants were positioned on their right side on a specially designed table with a small cut-out to allow for ultrasound imaging of the side of the femur that would impact the ground (Figure 3-3). To ensure participant comfort during imaging, a foam padding was added to the surface of the table and a pillow was placed between their knees (Figure 3-3 & Figure 3-4). Participants were asked to keep their knees and hips straight (no flexion) while ultrasound images were taken. Hip and knee positioning was standardized across participants to mitigate any potential influence of leg position on the dependent variables. This position was chosen as lateral falls with sideways landing configurations have the highest risk of resulting in a hip fracture (Nankaku et al., 2005; Yang et al. 2020). Previous studies measuring TSTT using ultrasound have positioned participants in either standing ((Lafleur, Benoit, 2016; Lafleur, Benoit R. et al., 2021; Levine et al., 2015; Maitland et al., 1993; Minns et al., 2007; Robinovitch et al., 1991), supine (Lafleur, Benoit, 2016; Lafleur, Benoit R. et al., 2021), or side-lying (Choi et al., 2015; Lafleur, Benoit, 2016; Lafleur, Benoit R. et al., 2021; Lim & Choi, 2021) positions while TSTT was measured. The previous studies that measured TSTT in a side-lying position measured it from the side of the body that would not impact the ground during a fall event. The positioning of participants during imaging in this thesis is the first to measure soft tissue thickness from the side of the femur that would impact the ground during a lateral fall.
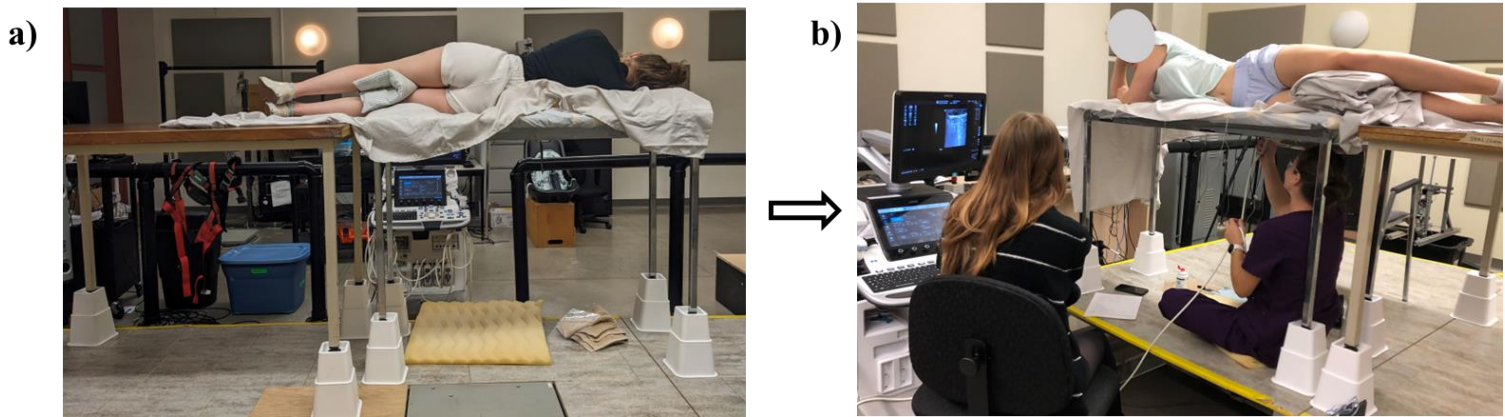
Figure 3-3: Participant positioning and lab setup. a) Shows the side-lying position all ultrasound images were taken in. Participants lie on their right side with their hips and knees straight. b) Shows the lab setup with a participant during a collection. Participants lay on their right side with their lateral proximal femur centered over the cut-out in the table. A pillow was placed between participants' knees to improve participant comfort. The primary investigator was positioned underneath of the table to ultrasound the lateral proximal femur. The table was placed on 9-inch-high risers to allow space for the primary investigator to sit beneath. A second investigator ran the ultrasound machine and adjusted image depth and gains as instructed by the primary investigator. When the primary investigator was satisfied with the image, the second investigator froze and then saved the image.

31
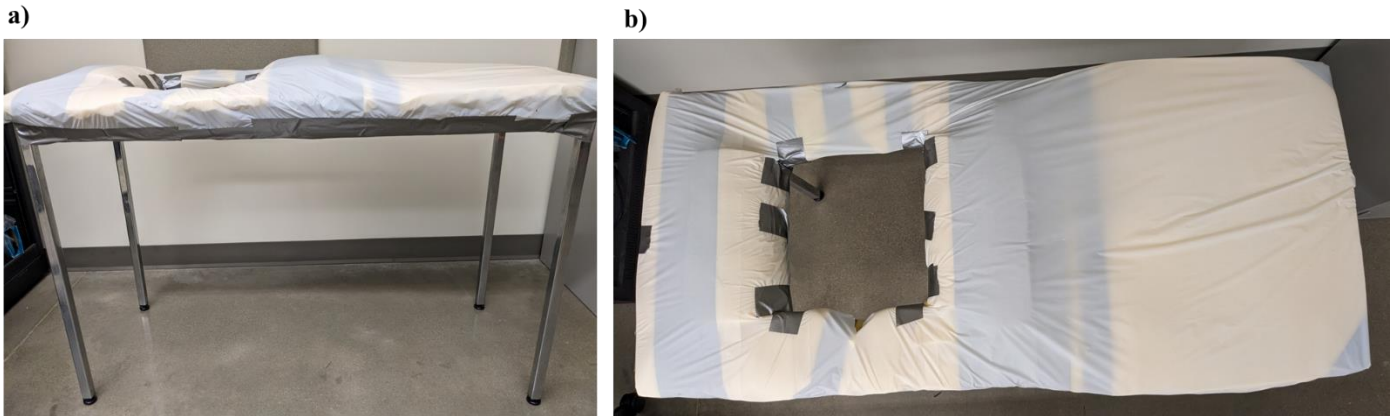
Figure 3-4: Shows the table with the cut-out. A waterproof cover was placed over the foam padding to allow for easy disinfection of the table between participants. a) Side view of the table. b) Bird's eye view of the table.

To assess regional differences in soft tissue thickness, ultrasound images were taken at 6 cm intervals throughout a 3 x 4 grid centered about the greater trochanter (Figure 3-5). To allow for use of the grid on participants, the grid was printed onto transparent and flexible projector paper and the holes were punched out post printing. This standardized grid means that different relative anatomical locations were assessed across participants. However, it was selected as it aligns with CSA Z325:20 for hip protectors, and hip protectors are of standardized sizes. There were four locations over the posterolateral aspect of the femur (P1, P2, P3, P4), four locations over the lateral aspect of the femur (L1, L2, L3, L4), and four locations over the anterolateral aspect of the femur (A1, A2, A3, A4). Point L2 was centered over the greater trochanter and the points below (points L3 and L4) were aligned with the diaphysis of the femur (Figure 3-5). This measurement grid was chosen as Pretty and colleagues (2021b; 2021a) found that peak pressure during a sideways fall is located distal and posterior to the GT.
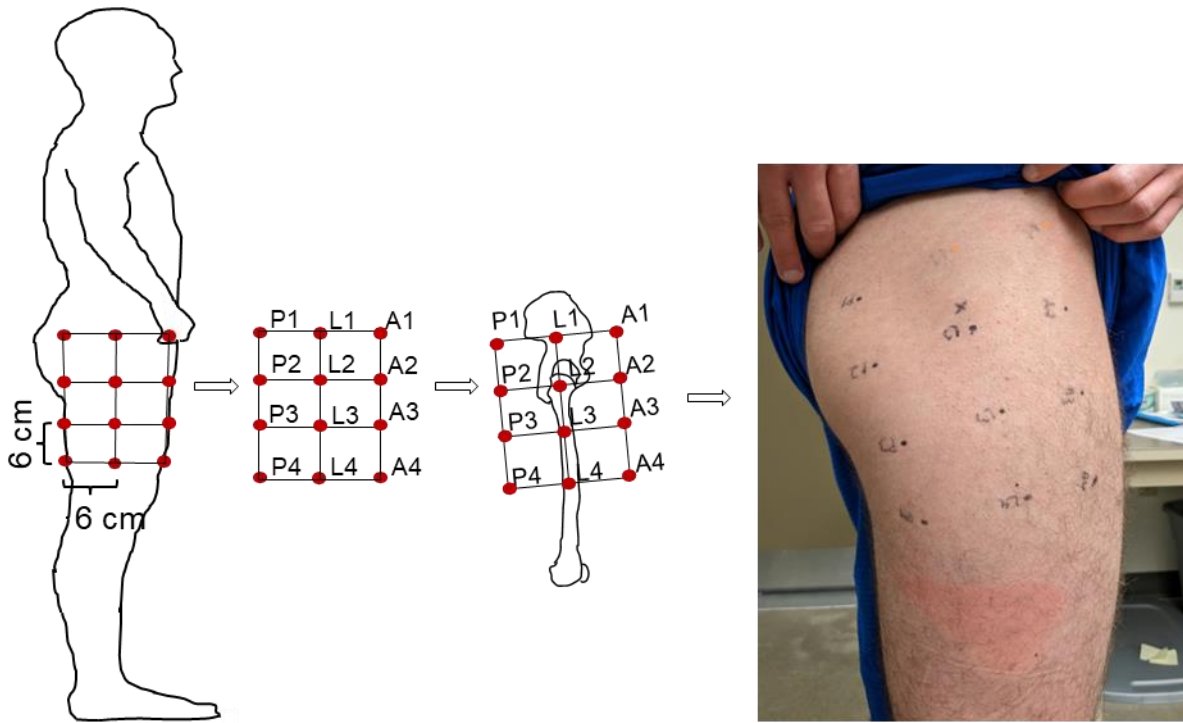
Figure 3-5: The location of the 12 measurement locations over the lateral proximal femur. Point L2 is positioned over the greater trochanter with points L3 and L4 aligned along the femur diaphysis. Measurement locations were spaced 6 cm apart.

To mark the imaging locations on participants, the investigator first manually palpated the GT, marking its location with indelible ink. This was done while participants were standing. Participants were then asked to get onto the table in the side-lying position with hips and knees straight. The ultrasound was then used to confirm that the mark was still centered over the greater trochanter. If the mark was not centered over the GT, the GT was located using the ultrasound and the skin marking was re-marked. The ultrasound was then used to image the diaphysis of the femur, with indelible ink being used to mark 3 – 4 points along it, distal to the GT. A small, flexible panel with a 3 by 4 grid of 0.5 cm diameter circular holes spaced 6 cm apart was used to mark the remaining imaging locations. The panel was placed over the participant's right femur so that point L2 was centered over the greater trochanter (location already marked) and the points below, points L3 and L4, were aligned with the diaphysis of the femur. This was done by placing L2 over the GT and aligning L3 and L4 with the points that were marked along the femur diaphysis. This method was used to ensure the orientation of the grid was consistent across participants. All remaining imaging points were then marked through

the holes in the panel with indelible ink and the panel was removed from participants. Participants were in the side-lying position while imaging locations were marked. This was done to mitigate potential movement and shifting of the soft tissues relative to the underlying femur, and therefore the imaging locations, as participants maneuvered into position for the experimental procedures. The specific order and steps taken to mark the imaging locations on participants can be found in Table 5.

Table 5: Description of the steps taken to mark the imaging locations on participants

Step Number	Instruction
Step 1	Palpate the GT while participant is standing and mark location with indelible ink.
Step 2	Position participant on the table in the side-lying position.
Step 3	Using the ultrasound, confirm the mark on the skin is still over the GT. If not, re-mark the GT location using ultrasound guidance.
Step 4	Use ultrasound to image the femur diaphysis. Ensure the probe is oriented to obtain transverse images and the femur diaphysis is centered in the middle of the image. Use indelible ink to mark 3 – 4 points along the femur diaphysis, distal to the GT. Markings were placed along the middle of the probe to ensure the center of the lateral femur diaphysis was used for landmarking.

Step 5	Place the measurement grid on the femur with L2 over the GT mark and L3 and L4 aligned along the marks on the femur diaphysis.
Step 6	Use indelible ink to mark all locations through the holes in the measurement grid.
Step 7	Remove the measurement grid from the participant. Label the locations on the skin surface with indelible ink.

B-mode ultrasound images were taken at each of the 12 imaging locations using the L2-9VN-D ultrasound probe. To mitigate the potential for muscle activation to influence the results (Levine et al., 2015), participants were instructed to stay as relaxed as possible while ultrasound images were taken. Transverse images were obtained with the probe oriented perpendicular to the participant's skin and such that posterior on the participant was on the left side of the ultrasound image. Care was taken to ensure the middle of the probe was aligned directly over the marked measurement location, to avoid compression of the soft tissues, and to ensure good visualization of the skin surface, subcutaneous adipose tissue, muscle, and the femur. Water-soluble ultrasound gel was applied to the probe as needed to increase the contact area between the surface of the skin and the ultrasound probe to improve the image quality. The penetration depth of the probe and gains of the ultrasound were

adjusted as necessary to obtain the best visualization of the above-mentioned structures. Once good visualization was achieved, the ultrasound image was saved, and the investigator moved on to the next imaging location. The primary investigator was responsible for maneuvering the ultrasound probe during imaging and for directing a second investigator to adjust image depth and gains as needed. The second investigator was responsible for freezing and saving the image when instructed to do so by the primary investigator. To mitigate the potential influence of imaging order and time spent in the side-lying position on the results, the order in which the locations were imaged was randomized using a random number generator. Three ultrasound images were taken at each imaging location, for a total of 36 images with the linear probe per participant. The specific steps taken when imaging locations can be found in Table 6.

Table 6: Description of the steps taken when imaging locations

Step Number	Instruction
Step 1	Apply water-soluble ultrasound gel to the surface of the ultrasound probe.
Step 2	Orient the ultrasound probe to obtain transverse ultrasound images, with the orientation marker on the probe on the posterior side of the participant (i.e. posterior on the participant corresponds to the left side of the ultrasound image).
Step 3	Place the middle of the ultrasound probe over the marking on the skin. Position the probe perpendicular to the skin surface and ensure that the probe is perpendicular to the long axis of the femur.
Step 4	Adjust the image depth and gains as necessary to obtain the best visualization of the femur, muscle, and adipose tissues. The second investigator was responsible for this as directed by the primary investigator.
Step 5	If required to visualize the femur, tilt the probe in anterior/posterior directions while ensuring the probe remains perpendicular to the long axis of the femur.
Step 6	Once good visualization of all structures is achieved, freeze the image, and then save it. The second investigator was responsible for this as directed by the primary investigator.

Following the ultrasound measurements, participant hip circumference, thigh circumference around row 4 of the grid, the distance between the iliac crest and L1, the vertical (y) distance between the ASIS and L1, and the horizontal (x) distance between the ASIS and L1 were measured. The resultant distance between the ASIS and L1 was calculated using the x,y measurements and the following formula:

$$ASIS \text{ to } L1 \text{ resultant} = \sqrt{(ASIS \text{ to } L1x)^2 + (ASIS \text{ to } L1y)^2}$$

3.1.5 Data Analysis

The dependent variables in this study are TST, MT, and AT. TST is a measure of the combined thicknesses of the skin, muscle, and subcutaneous adipose tissue overlying the femur. For the purposes of this study, and similar to Lafleur and colleagues (2021), TST is defined as the distance between the outer edge of the femur and the outer edge of the skin (Figure 3-6). MT is a measure of the thickness of the muscle overlying the femur and is defined as the distance between the outer edge of the femur and the outer edge of the muscle fascia (Figure 3-6). MT measurements may include the thickness of tendon, bursa, and intramuscular fat in addition to muscle fibers and fascia. AT is a measure of the thickness of the subcutaneous adipose tissue and is defined as the distance between the outer edge of the muscle fascia and the inner edge of the skin (Figure 3-6).

Figure 3-6: Transverse plane ultrasound images of P3, L3, and A3 Total soft tissue thickness is represented by the white arrow (A), subcutaneous adipose tissue thickness is represented by the orange arrow (B), and muscle thickness is represented by the red arrow (C). All measurements are taken along the straight line directly underneath the skin surface marker.

TST, MT, and AT were measured using the built-in measurement function of the ultrasound software (General Electric Company, version R1, revision 5.2, software part number 5821700-8) (Figure 3-7). These variables were measured after the data collection session was finished. For all locations, thickness measurements were taken from the middle of the ultrasound image straight down to the underlying landmark of interest as the center of the probe was placed over the marked location on the participant's skin (Figure 3-6). This method for measuring soft tissue thickness provides the thickness of the soft tissues lying directly under the measurement point on the skin. TST was measured from the skin surface in the middle of the image straight down to the underlying femur. MT was measured in the middle of the image from the outer edge of the muscle fascia to the outer edge of the femur. AT was measured from the middle of the image from the outer edge of the muscle fascia to the inner edge of the skin.
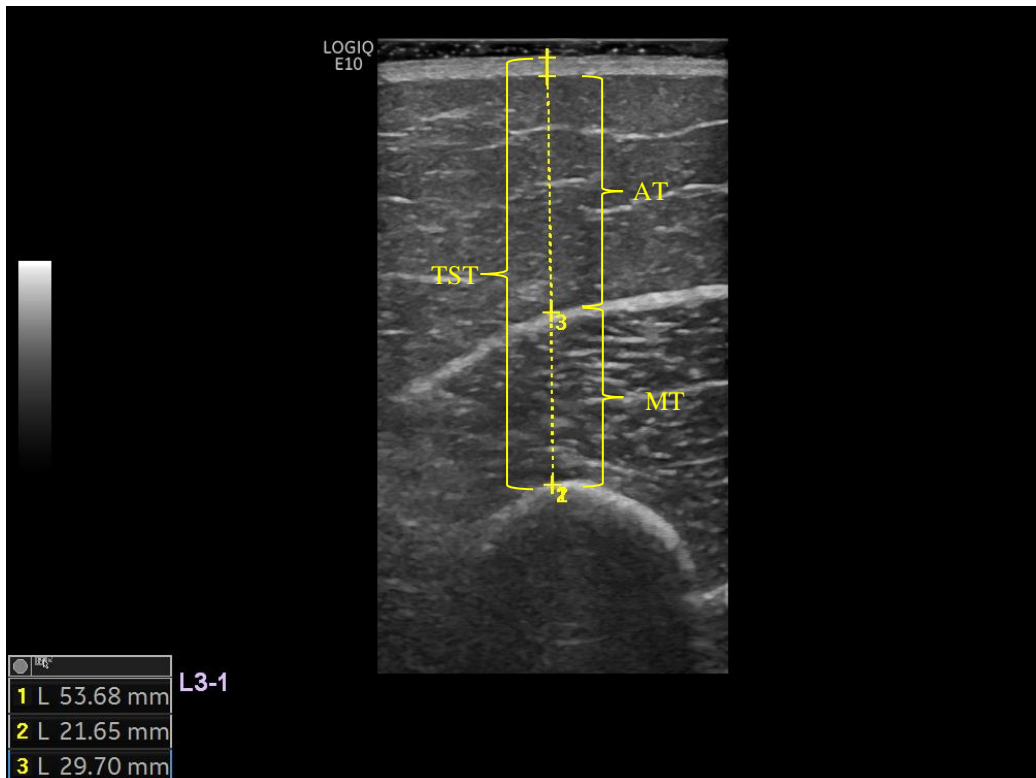
Figure 3-7: The built-in measurement function of the GE ultrasound. The numbers in the bottom left corner of the image indicate thickness measurements (in mm) of TST (1), MT (2), and AT (3). Numbers along the yellow dotted line correspond to the measurement caliper's starting point for each thickness measurement. When looking along the yellow dotted line, TST is the distance between #1 and the caliper marker on the outer edge of the skin (i.e. the distance between the outer surface of the femur to the outer edge of the skin), MT is the distance between #2 and #3 (i.e. the distance between the outer edge of the femur to the outer edge of the muscle, and AT is the distance between #3 and the caliper marker on the inner edge of the skin (i.e. the distance between the outer edge of the muscle and the inner edge of the skin). Because TST and MT have the same starting point, their respective number markers on the image overlap, and only #2, which is the starting point for the MT measurement, is clearly visible.

3.1.6 Statistical Analysis

3.1.6.1 Sample Size Calculation

Based on sample size calculations, a sample size of 12 (6 males and 6 females) was needed to achieve 80% power for observing differences in TST between males and females ($\alpha = 0.05$, effect size d = 1.55 ((Lafleur, Benoit, 2016); GPower 3.1.9.7, Universität Düsseldorf, Düsseldorf, Germany). However, differences in TST between some measurement locations may not be as pronounced and it

is less clear in the literature what the effect sizes for sex will be for muscle and adipose tissue thickness. To account for this, a sample size of 25 (12 males and 13 females) was used in this study. By increasing the sample size to 25, the power to detect differences in TST based on sex increased to 98.3%.

3.1.6.2 Statistical Analysis

For each hypothesis, a separate statistical analysis was performed in SPSS (IBM SPSS Statistics 28.0.1).

Hypotheses 1 and 2 assessed the intra-rater reliability of the protocol. Specifically, the intra-rater reliability of probe repositioning, image acquisition, and image analysis were tested.

For hypothesis 1, a two-way mixed effects absolute agreement intraclass correlation (ICC) model was used to assess intra-rater reliability for TST, MT, and AT. ICCs were calculated for TST, MT, and AT separately at each of the 12 measurement locations. Individual ICCs were compared to the Koo & Li's (2016) classification approach of poor (ICC < 0.5), moderate (ICC between 0.5 – 0.75), good (ICC between 0.75 – 0.9), or excellent (ICC > 0.9). Standard error of measurement (SEM), was also calculated for TST, MT, and AT. SEM was calculated for TST, MT, and AT at each of the 12 measurement locations. SEM was calculated based on the following equation (Weir, 2005):

$$SEM = \sqrt{mean\ square\ error})$$

The minimum difference (MD) to be considered real was then calculated based on the SEM using the following equation from Weir (2005):

$$MD = SEM \times 1.96 \times \sqrt{2}$$

For hypothesis 2, the ICCs calculated for hypothesis 1 were rank-ordered and classified as poor (ICC < 0.5), moderate (ICC between 0.5 – 0.75), good (ICC between 0.75 – 0.9), and excellent (ICC > 0.9) (Koo & Li, 2016). From a statistical difference perspective, the 95% confidence intervals of the ICCs at each location were compared. Reliability between locations was considered different if:

1) ICC values fell into different classification categories; or

2) there was no overlap between the 95% CI across different locations.

This exercise was performed separately for dependent variables TST, MT, and AT.

For hypotheses 3 and 4, two-way mixed model ANOVAs were performed separately for TST, MT, and AT with sex (male, female) as a between groups factor and measurement location (12 locations) as a within groups factor. The 12 individual measurement locations were then combined into 3 locations based on their location relative to the femur. Measurements taken at P1, P2, P3, P4 were averaged together to form the posterolateral location. Measurements taken at L1, L2, L3, L4 were averaged together to form the lateral location. Measurements taken at A1, A2, A3, A4 were averaged together to form the anterolateral location. A second two-way mixed model ANOVA was then performed separately for TST, MT, and AT with sex (male, female) as a between groups factor and measurement location (posterolateral, lateral, anterolateral) as a within groups factor. For hypothesis #3 the main effect of sex was examined for TST, MT, and AT. For hypothesis 4, the main effect of location was examined. If significant effects were observed, conditions which were different from one another were determined through post-hoc pairwise comparisons with a Bonferroni correction applied.

While interactions were not expected based on the hypotheses, if they did emerge further interpretation steps would have been taken. If the interactions were ordinal in nature, main effects were interpreted. If they were disordinal, interactions were decomposed separately using one-way ANOVA to examine the influence of location for each sex, or paired t-tests to examine the influence of sex at each location.

Prior to ANOVA, data were checked for normality using the Shapiro-Wilk test and homogeneity of variance using Levene's test. Mauchly's test was used to test the assumption of sphericity and Huyn-Feld epsilon corrections were employed if the assumption of sphericity was violated.

3.2 Results

3.2.1 Participant Characteristics

A summary of participant characteristics and anthropometrics can be found in Table 7. For a visual depiction of the location of the measurement grid relative to the average location of the ASIS and the iliac crest, refer to Figure 3-8.

Table 7: Descriptive statistics for all participants. Values presented are mean (SD).

	Total (n = 25)	Males (n = 12)	Females (n = 13)
Age (years)	20.8 (1.86)	21.5 (2.02)	20.2 (1.54)
BMI (kg/m^2)	22.56 (2.99)	23.62 (3.35)	21.59 (3.27)
Hip Circumference (cm)	97.7 (5.66)	98.3 (4.78)	97.0 (6.68)
Thigh Circumference at Row 4 (cm)	56.4 (4.37)	57.2 (3.86)	55.5 (4.88)
Iliac Crest to L1 Distance (cm)	13.1 (2.36)	13.4 (2.1)	12.8 (2.7)
ASIS to L1 y Distance (cm)	7.5 (1.86)	7.5 (1.29)	7.5 (2.4)
ASIS to L1 x Distance (cm)	10.5 (1.87)	10.5 (2.29)	10.4 (1.38)
ASIS to L1 Resultant Distance (cm)	12.9 (1.97)	12.9 (1.97)	12.9 (2.07)
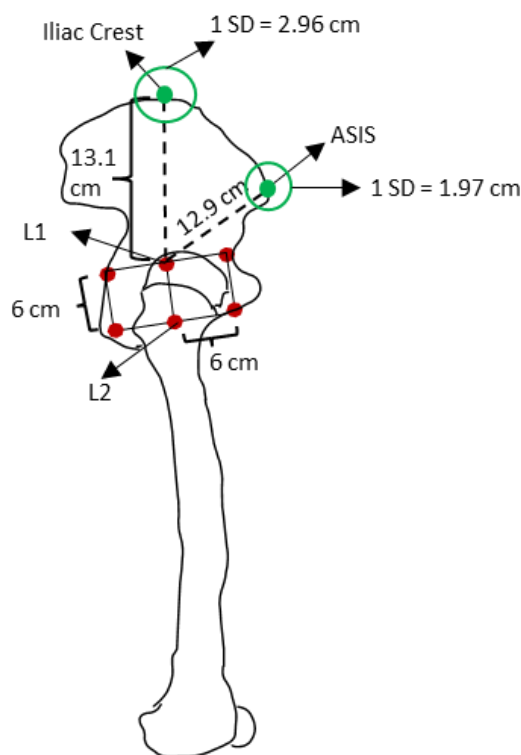
Figure 3-8: Demonstrates the average location of the iliac crest and ASIS relative to the measurement grid. The bottom two rows of the grid have been removed for the sake of image clarity. Point L2 is directly over the greater trochanter. Green circles surrounding the average iliac crest and ASIS locations represent one standard deviation in location.

3.2.2 Reliability

3.2.2.1 General Reliability Trends

ICCs were good or excellent across all tissue types and locations, except for muscle thickness at P1, muscle thickness at A1, total thickness at P1, and total thickness at A1 (Figure 3-9). ICCs ranged from 0.486 for muscle at A1 to 0.994 for adipose at L4 (Table 8), with average (SD) ICCs being 0.89 (0.13) across all tissue types and locations. Average (SD) ICCs for muscle thickness, adipose thickness, and total thickness were 0.85 (0.15), 0.95 (0.03), and 0.87 (0.15) respectively. Standard error of the measurement across measurement locations can be seen in Figure 3-10.

43
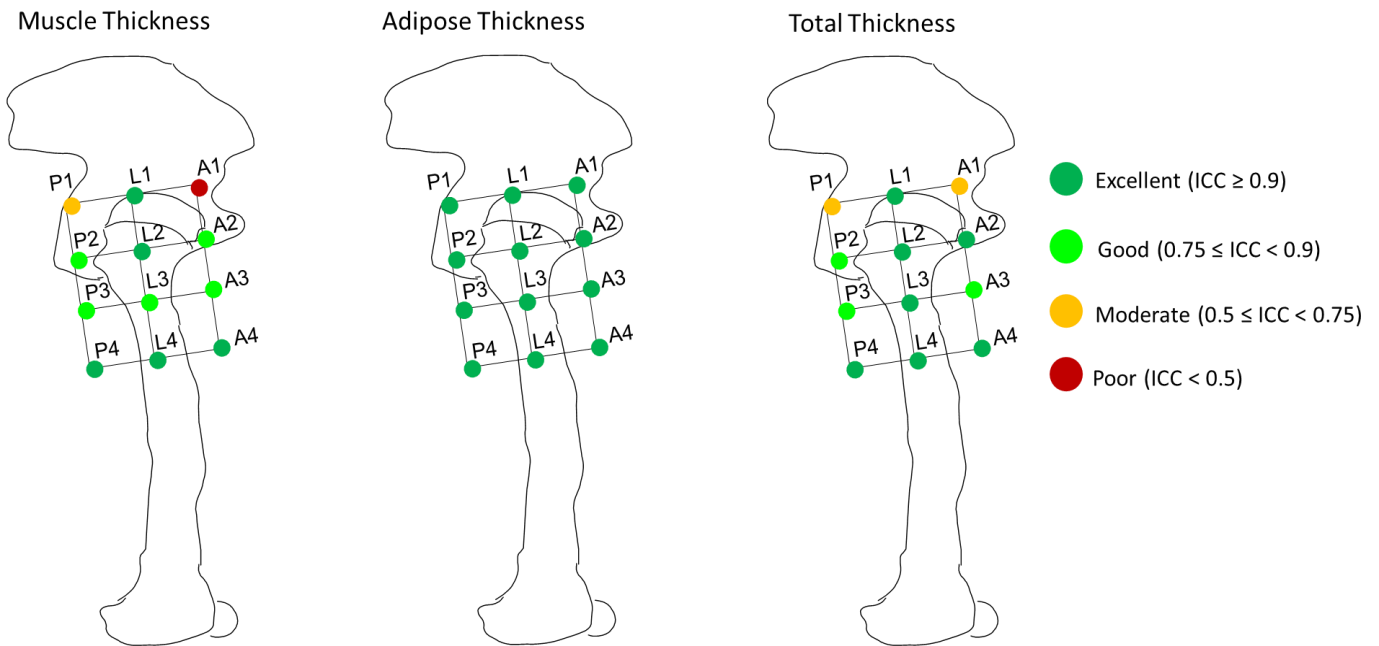
Figure 3-9: Visual representation of ICCs for all tissue types and locations. Koo & Li's 2016 guidelines for reporting ICCs were used to classify ICCs as poor, moderate, good, or excellent. ICCs were classified as good or excellent for all locations and tissue types, except for muscle thickness at both P1 and A1, and total thickness at both P1 and A1.
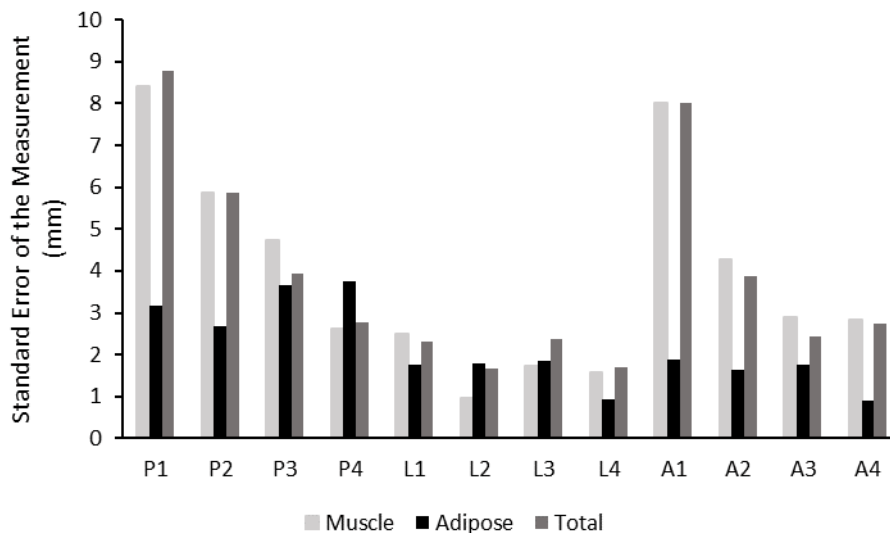
Figure 3-10: Standard error of the measurement for all tissue types across all measurement locations.

3.2.2.2 Differences in Reliability

Rank-ordered ICCs for all tissue types and locations can be seen in Table 8. Based on ICC classification and confidence interval overlap, measures of muscle and total soft tissue thickness at P1 and A1 measurement locations were significantly less reliable than all other tissue thickness measurements across all locations. ICCs for adipose thickness across all locations was excellent, and there were no differences in reliability of adipose measurements across locations (Figure 3-11).

Table 8: Rank-ordered intraclass correlation coefficients for all measurement locations and tissue types. ICCs were classified as poor, moderate, good, or excellent based on Koo & Li's (2016) guidelines for reporting ICCs. Row colours provide a visual representation of the calculated ICC value, with red being poor reliability, yellow being moderate, light green being good, and darker green being excellent. Standard error of the measurement is also presented.

Tissue Type	Location	Cronbach's Alpha	Single Measures ICC	Single Measures 95% CI Lower Bound	Single Measures 95% CI Upper Bound	p value	Koo & Li's Classification	Standard Deviation (mm)	Mean Square Error	Standard Error of the Measurement (mm)	Minimum Difference to be Considered Real (mm)
Muscle	A1	0.744	0.486	0.25	0.702	<0.001	Poor	11.217	64.287	8.018	22.225
Muscle	P1	0.817	0.593	0.374	0.775	<0.001	Moderate	13.201	70.826	8.416	23.327
Muscle	P3	0.944	0.853	0.738	0.927	<0.001	Good	11.992	22.478	4.741	13.142
Muscle	P2	0.948	0.863	0.755	0.932	<0.001	Good	15.470	34.455	5.870	16.270
Muscle	A2	0.959	0.879	0.781	0.94	<0.001	Good	12.539	18.244	4.271	11.839
Muscle	L3	0.958	0.887	0.795	0.945	<0.001	Good	4.987	2.982	1.727	4.787
Muscle	A3	0.962	0.888	0.796	0.945	<0.001	Good	8.874	8.452	2.907	8.058
Muscle	L4	0.967	0.908	0.832	0.955	<0.001	Excellent	5.117	2.508	1.584	4.390
Muscle	A4	0.967	0.908	0.832	0.955	<0.001	Excellent	9.211	8.046	2.837	7.863
Muscle	L1	0.982	0.949	0.905	0.975	<0.001	Excellent	10.824	6.274	2.505	6.943
Muscle	P4	0.991	0.971	0.944	0.986	<0.001	Excellent	16.056	6.905	2.628	7.284
Muscle	L2	0.993	0.979	0.959	0.99	<0.001	Excellent	6.433	0.938	0.969	2.685
Adipose	P4	0.966	0.906	0.829	0.954	<0.001	Excellent	12.031	14.027	3.745	10.381
Adipose	P1	0.972	0.911	0.83	0.957	<0.001	Excellent	11.169	10.006	3.163	8.768
Adipose	A1	0.972	0.914	0.839	0.958	<0.001	Excellent	6.665	3.588	1.894	5.250
Adipose	A2	0.976	0.928	0.866	0.965	<0.001	Excellent	6.177	2.726	1.651	4.577
Adipose	P3	0.983	0.945	0.894	0.974	<0.001	Excellent	16.345	13.308	3.648	10.112
Adipose	P2	0.988	0.965	0.933	0.983	<0.001	Excellent	13.765	7.103	2.665	7.387
Adipose	A3	0.99	0.968	0.939	0.985	<0.001	Excellent	9.975	3.092	1.758	4.874
Adipose	L1	0.991	0.973	0.949	0.987	<0.001	Excellent	10.726	3.122	1.767	4.898
Adipose	L3	0.993	0.981	0.963	0.991	<0.001	Excellent	13.043	3.446	1.856	5.146
Adipose	L2	0.994	0.982	0.966	0.992	<0.001	Excellent	13.020	3.170	1.780	4.935
Adipose	A4	0.997	0.99	0.981	0.995	<0.001	Excellent	8.790	0.794	0.891	2.470
Adipose	L4	0.998	0.994	0.989	0.997	<0.001	Excellent	11.970	0.878	0.937	2.597
Total	A1	0.804	0.56	0.334	0.752	<0.001	Moderate	12.345	64.125	8.008	22.197
Total	P1	0.823	0.583	0.359	0.768	<0.001	Moderate	14.072	76.841	8.766	24.298
Total	P2	0.945	0.854	0.74	0.927	<0.001	Good	14.999	34.521	5.875	16.286
Total	P3	0.953	0.858	0.744	0.93	<0.001	Good	10.828	15.482	3.935	10.906
Total	A3	0.953	0.873	0.772	0.937	<0.001	Good	6.743	5.993	2.448	6.786
Total	A2	0.967	0.903	0.823	0.953	<0.001	Excellent	12.549	15.023	3.876	10.744
Total	A4	0.966	0.906	0.828	0.954	<0.001	Excellent	8.812	7.530	2.744	7.606
Total	P4	0.988	0.961	0.926	0.982	<0.001	Excellent	14.462	7.755	2.785	7.719
Total	L1	0.988	0.965	0.934	0.983	<0.001	Excellent	12.310	5.393	2.322	6.437
Total	L3	0.99	0.971	0.945	0.986	<0.001	Excellent	13.655	5.676	2.382	6.604
Total	L4	0.992	0.978	0.95	0.989	<0.001	Excellent	11.160	2.915	1.707	4.732
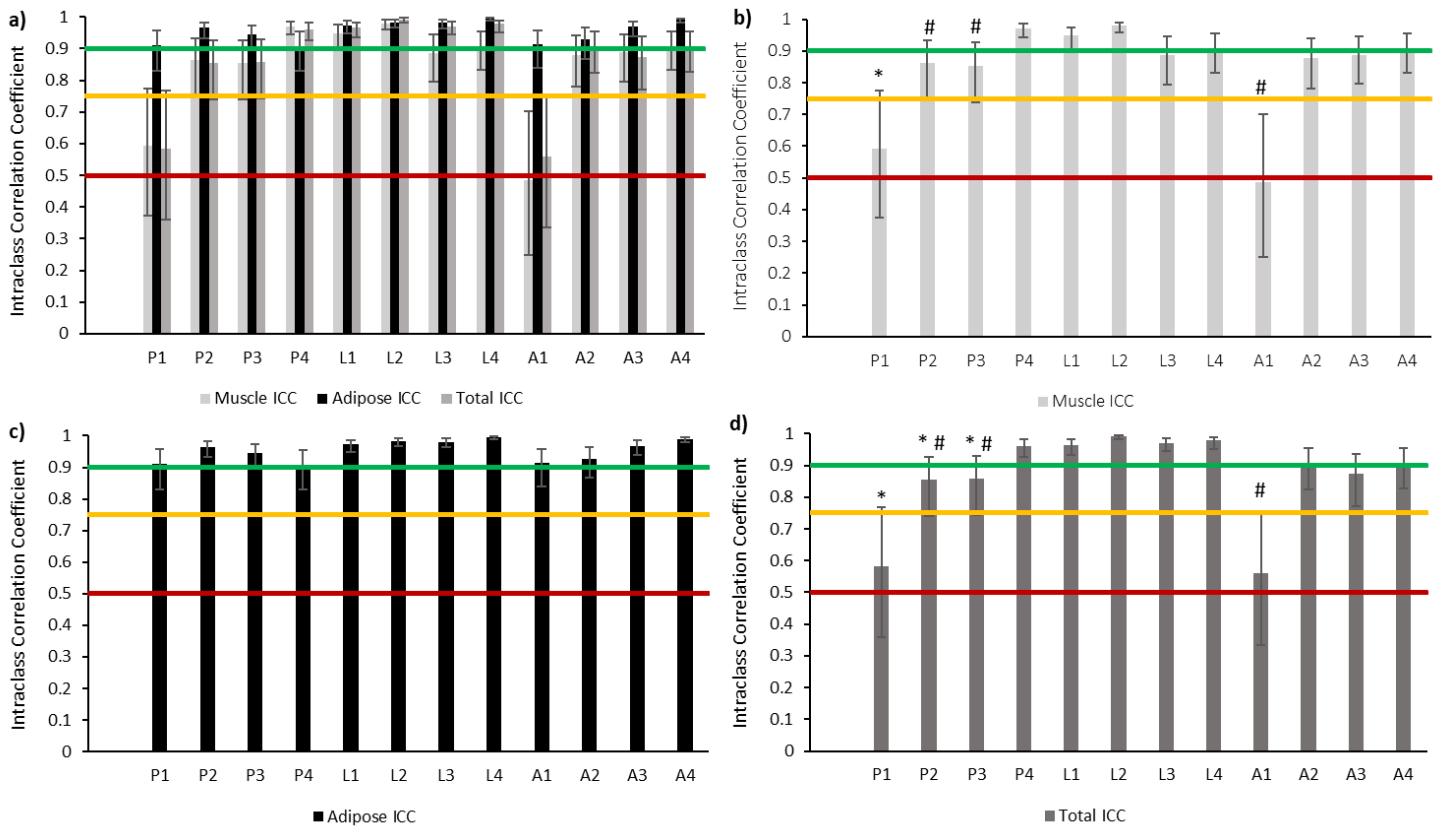
Figure 3-11: Intraclass correlation coefficients for soft tissue thickness measurements. Error bars represent the 95% confidence intervals. Values above the red line have reached a moderate ICC (ICC > 0.5). Values above the orange line have reached a good ICC (ICC > 0.75). Values above the green line have reached an excellent ICC (ICC > 0.9). Reliability was good to excellent for all locations and tissue types except for measures of muscle and total thickness at locations P1 and A1. For muscle and total thickness graphs, * indicate reliability is not significantly different from A1 based on overlap between 95% confidence intervals and # indicate reliability is not significantly different from P1 based on overlap between 95% confidence intervals. a) Shows ICCs for all tissue types and locations. b) Shows ICCs for measurements of muscle thickness. c) Shows ICCs for adipose thickness. There are no differences in reliability between locations. d) Shows ICCs for total soft tissue thickness.

3.2.3 Soft Tissue Thickness and Composition

3.2.3.1 General Soft Tissue Thickness Trends

The thickness of muscle, adipose, and total soft tissues varied across the 12 measurement locations and between males and females (Figure 3-12). The average (SD) for muscle thickness ranged from 8.34 (6.43) mm at L2 to 52.27 (11.22) mm at A1. The average (SD) for adipose thickness ranged from 10.28 (6.66) mm at A1 to 30.02 (16.05) mm at P3. The average (SD) for total soft tissue thickness ranged from 31.38 (16.78) mm at L2 to 75.98 (14.07) mm at P1.

The average (SD) muscle thickness for males ranged from 7.25 (2.91) mm at L2 to 54.1 (8.59) mm at A3. For adipose, thicknesses ranged from 7.37 (5.17) mm at A1 to 24.3 (15.0) mm at P3. For total soft tissues, thicknesses ranged from 22.7 (10.7) mm at L2 to 73.8 (11.8) mm at P1. For females, the average (SD) for muscle thickness ranged from 9.32 (8.44) mm at L2 to 51.4 (9.15) mm at A2. For adipose tissue, thicknesses ranged from 13.9 (9.55) mm at A2 to 37.9 (14.7) mm at P3. Total soft tissue thickness ranged from 39.1 (17.3) mm at L2 to 83.2 (15.0) mm at P1.
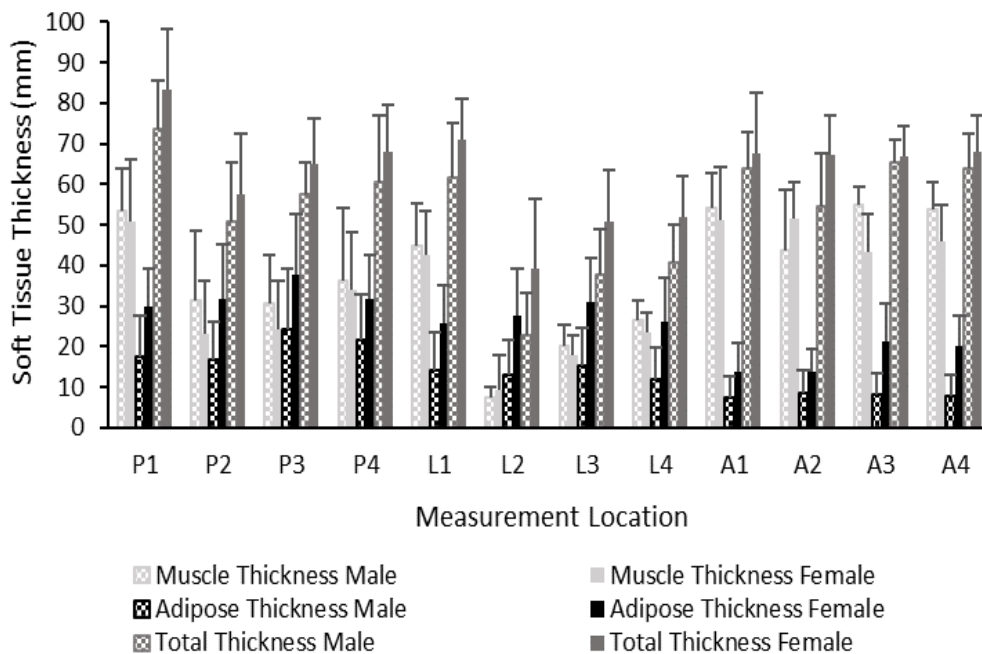
Figure 3-12: Soft tissue thickness for each tissue type across the 12 measurement locations, separated by sex. Error bars represent standard deviation.

When normalized to TST, muscle and adipose thickness also varied (Figure 3-13). Muscle accounted for only 28.7 % of TST at L2 and 80.6 % of TST at A1 while adipose accounted for 15.9% of TST at A1 and 61.5 % of TST at L2. The ratios of muscle and adipose tissues to total soft tissue thickness also varied by sex. For males, we saw that muscle accounted for 33.9% of TST at L2 and 85.1% of TST at A1 while adipose accounted for 11.0% of TST at A1 and 53.5% of TST at L2. For females, we saw that muscle accounted for 23.4% of TST at L2 and 76.7% of TST at A2 while adipose accounted for 20.3% of TST at A2 and 69.6% of TST at L2.
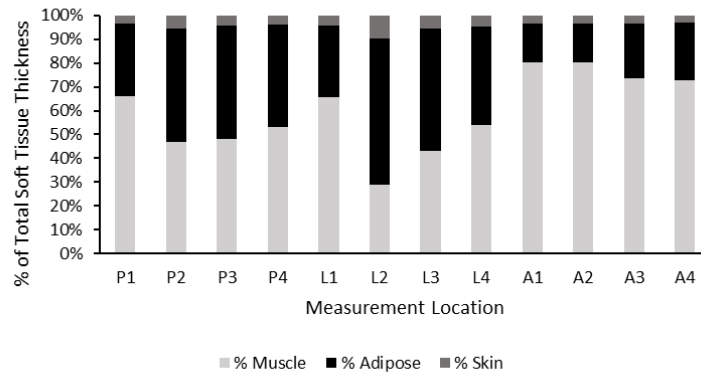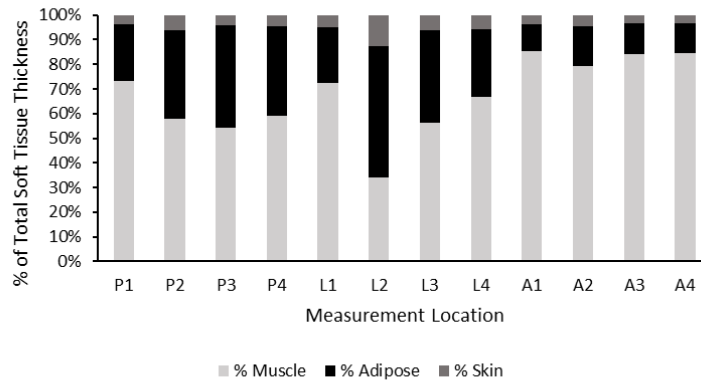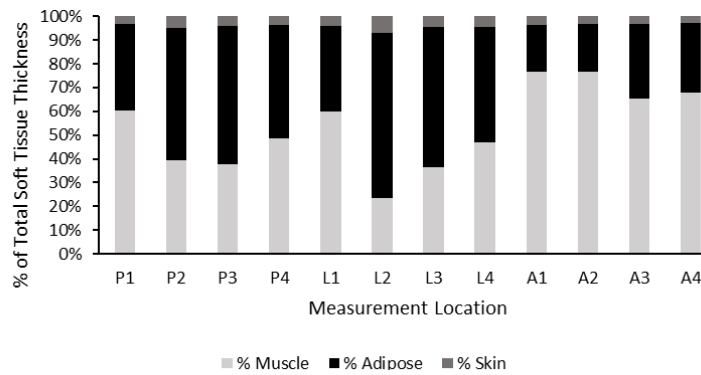
Figure 3-13: Percent contribution of muscle, adipose, and skin thickness to total soft tissue thickness. a) Percent contribution each tissue type for male and female data combined. b) Percent contribution of each tissue type for males. c) Percent contribution of each tissue type for females.

3.2.3.2 Overall ANOVA Results

A general summary of the two-way mixed model ANOVA results is presented below. These results will be explored further in sections 3.2.3.3 and 3.2.3.4.

3.2.3.2.1 Two-Way Mixed Model ANOVA with Sex and Twelve Separate Measurement Locations (Figure 3-12):

There was no significant interaction between sex and measurement location for any of the tissue types (MT: $F = 1.151$, $p = 0.337$; AT: $F = 1.844$, $p = 0.113$; TST: $F = 1.922$, $p = 0.062$). There were significant main effects of both sex and location for muscle (sex: $F = 4.989$, $p < 0.001$; location: $F = 54.293$, $p < 0.001$), adipose (sex: $F = 15.155$, $p < 0.001$; location: $F = 22.573$, $p < 0.001$), and total soft tissue thickness (sex: $F = 6.19$, $p = 0.021$; location: $F = 52.359$, $p < 0.001$).

3.2.3.2.2 Two-Way Mixed Model ANOVA with Sex and Three Separate Measurement Locations (Figure 3-14):

Once the measurement locations were combined into posterolateral, lateral, and anterolateral locations, the ANOVA revealed no significant interaction between sex and measurement location for muscle and adipose thicknesses (MT: $F = 0.269$, $p = 0.673$; AT: $F = 1.744$, $p = 0.195$). There was a significant interaction between sex and measurement location for total soft tissue thickness (Figure 3-15), however this interaction was ordinal in nature and main effects were interpreted ($F = 4.229$, $p = 0.021$). Significant main effects of sex and measurement location were observed for all tissue types (MT: sex $F = 4.698$, $p < 0.041$; location $F = 85.598$, $p < 0.001$; AT: sex $F = 15.155$, $p < 0.001$; location $F = 42.272$, $p < 0.001$; TST: sex $F = 6.19$, $p = 0.021$, location $F = 92.088$, $p < 0.001$).
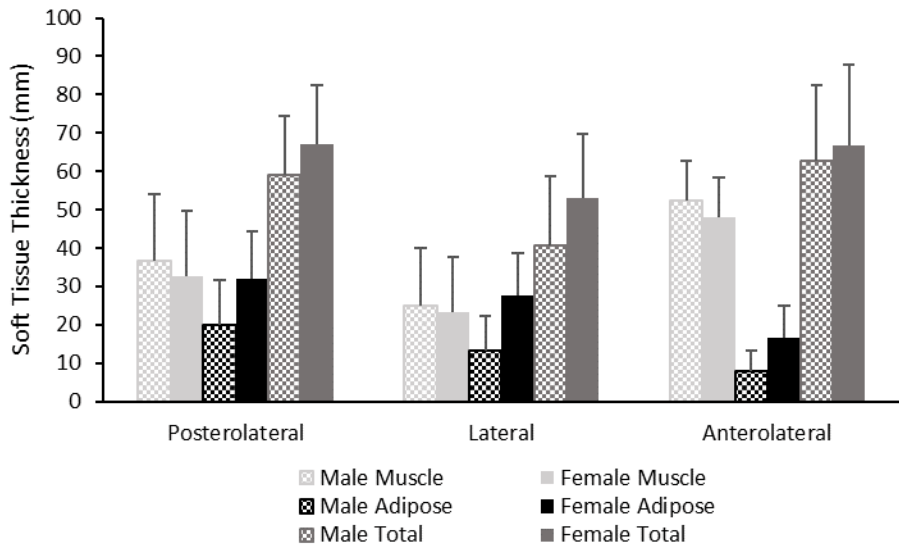
Figure 3-14: Soft tissue thickness across the three measurement locations, separated by sex. Error bars represent standard deviation.
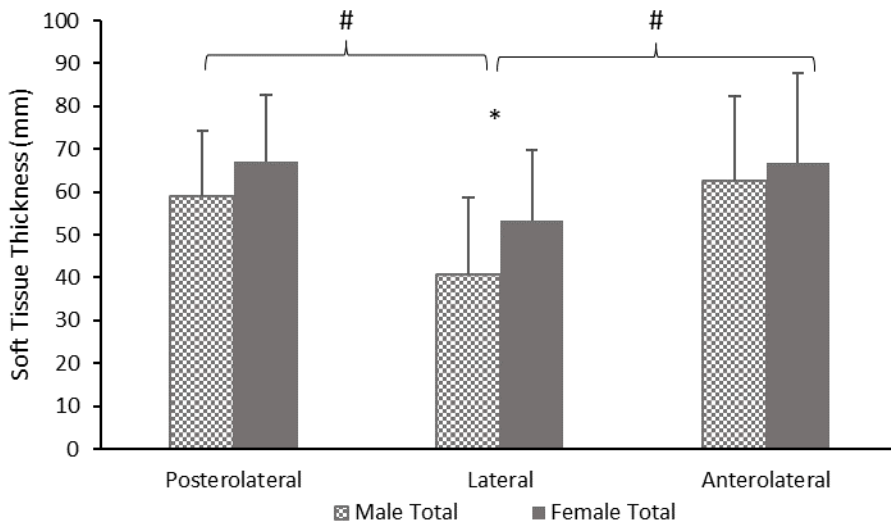
Figure 3-15: Interaction between sex and measurement location for total soft tissue thickness. * indicates significant differences between males and females within a location. # indicate significant differences between locations for each sex.

3.2.3.3 Effect of Sex on Soft Tissue Thickness and Composition

As previously stated in section 3.2.3.2, ANOVA revealed significant main effects of sex for all tissue types. Post-hoc pairwise comparisons revealed that males had significantly more muscle, less adipose, and less total soft tissues than females (all $p < 0.05$, Figure 3-16).
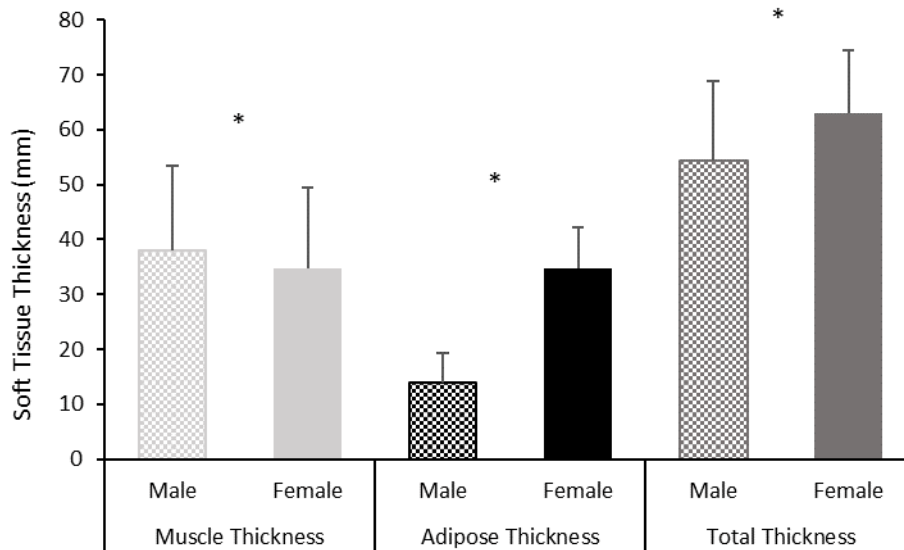
Figure 3-16: Main effect of sex on soft tissue thickness. * indicate significant differences between males and females within a tissue type (all p < 0.05).

3.2.3.4 Effect of Measurement Location on Soft Tissue Thickness and Composition

As previously stated in section 3.2.3.2, the initial ANOVA investigating the influence of sex and 12 measurement locations revealed no significant interactions between sex and measurement location for any of the tissue types, and a significant main effect of location for all tissue types. The post-hoc ANOVA with locations grouped into posterolateral, lateral, and anterolateral locations revealed a significant ordinal interaction between sex and measurement location for total soft tissue thickness (Figure 3-15), and significant main effects of location for all tissue types (Figure 3-17).

Post-hoc pairwise comparisons revealed that muscle thickness was significantly larger over the anterolateral femur compared to both the posterolateral and lateral femur ($p < 0.001$), and muscle thickness over the posterolateral femur was significantly larger than over the lateral femur ($p < 0.001$,

Figure 3-17). Adipose thickness was significantly larger over the posterolateral femur compared to both the lateral femur ($p = 0.008$) and the anterolateral femur ($p < 0.001$), and adipose thickness was significantly larger over the lateral femur compared to the anterolateral femur ($p < 0.001$, Figure 3-17). Total soft tissue thickness was significantly larger over the anterolateral and posterolateral femur compared to the lateral femur (both $p < 0.001$), with no significant difference in total soft tissue thickness between the anterolateral and posterolateral femur ($p = 1.00$, Figure 3-17).
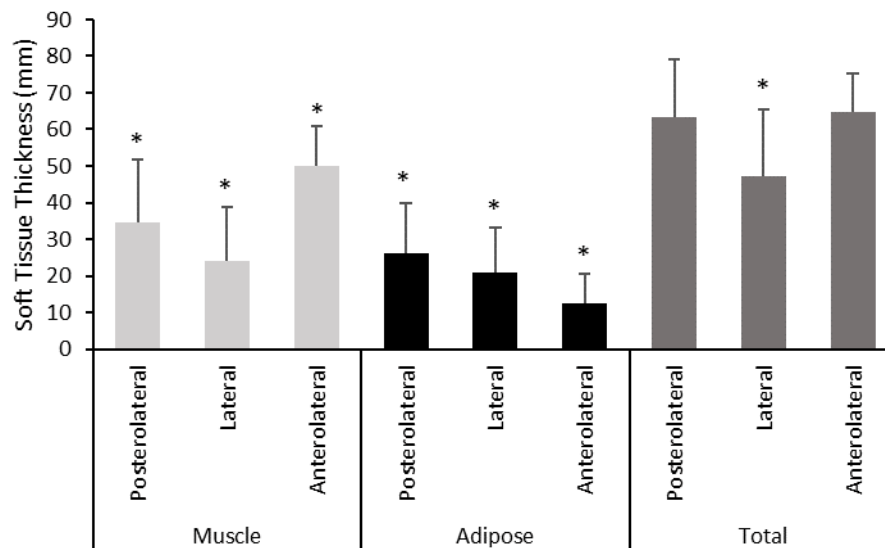
Figure 3-17: Main effect of location on soft tissue thickness over the femur. Error bars represent standard deviation. * indicate significant differences between locations within a tissue type (all p < 0.05).

As previously stated in section 3.2.3.2, there was a significant main effect of location for all tissue types when looking at the 12 separate measurement locations. Post-hoc comparisons with L2 (point directly over the GT) revealed location-based differences for all three tissue types (Figure 3-18). Muscle thickness at L2 is significantly lower than any of the other 11 measured locations (all $p < 0.001$), adipose thickness at L2 is significantly lower than the four locations over the anterolateral femur (A1 – A4, all $p < 0.05$), and total soft tissue thickness at L2 is significantly lower than any of the other 11 measured locations (all $p < 0.001$).

53
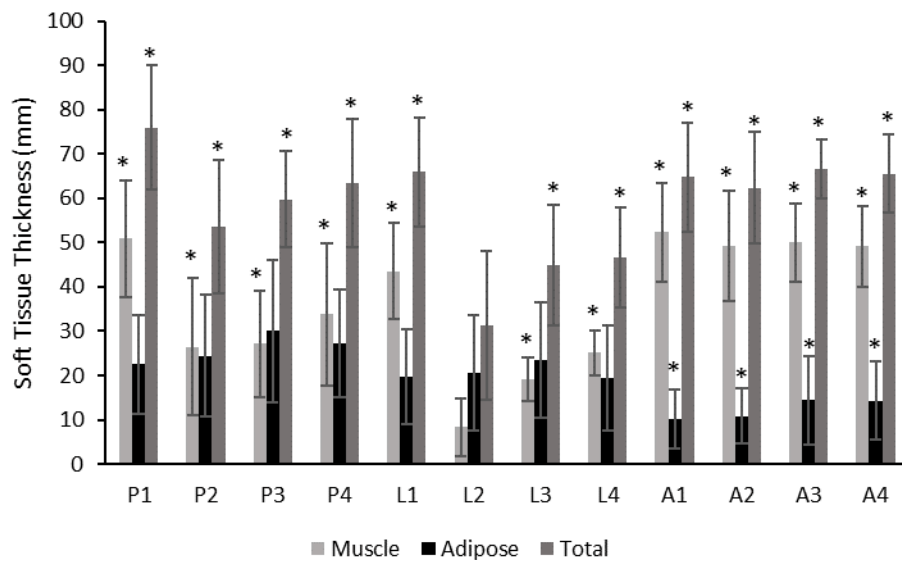
Figure 3-18: Main effect of location across the L2 measurement locations. Muscle and total soft tissue thickness at all locations was significantly different than L2, while adipose thickness over the four anterolateral locations was significantly different than L2. * indicate significant differences from L2 within a tissue type (all p < 0.05).

3.3 Discussion

The overall goals of this thesis were to assess the intra-rater reliability of ultrasound measured soft tissue thickness (muscle, adipose, and total) over 12 locations on the proximal femur and to assess differences in the thickness of these tissues based on measurement location and sex. Regarding hypothesis one, the data demonstrated reliable measures of muscle, adipose, and total soft tissue thickness (ICCs > 0.85) at all locations except for muscle and total thicknesses at A1 and P1 locations (ICCs < 0.6). Regarding the second hypothesis, the data demonstrated differences in reliability based on measurement location, with measurements at A1 and P1 being less reliable than other locations. However, this finding only holds true for muscle and total soft tissue thickness measurements. There were no location-based differences in reliability for adipose thickness measurements. In line with hypothesis three, the data showed that males have more muscle, less adipose, and less total soft tissues than females. Finally, in line with hypothesis four, the data showed that adipose thickness over the posterolateral femur was greater than the lateral femur which was greater than the anterolateral

femur. For muscle thickness, hypothesis four was partially supported with muscle thickness being lowest over the lateral femur. However, muscle thickness was greatest over the anterolateral femur instead of the posterolateral femur. For total soft tissues, hypothesis four was also partially supported with total thickness being lowest over the lateral femur. However, no differences were seen between the posterolateral and anterolateral femur. For thicknesses relative to the GT, hypothesis four was supported with thicknesses of all tissues being lowest over the GT.

3.3.1 Intra-Rater Reliability

Our reliability outcomes generally support the ability of this protocol to explore potential sex and location effects on soft tissue thickness outcomes over the proximal femur. Across locations, ICCs were on average (SD) 0.847 (0.15) for muscle, 0.955 (0.03) for adipose, and 0.867 (0.15) for total soft tissues. ICCs ranged between 0.486 – 0.979 for muscle, 0.906 – 0.994 for adipose, and 0.56 – 0.991 for total soft tissue thickness. Reliability was generally similar between measurements of muscle and total soft tissue thickness, and better for measurements of adipose compared to both muscle and total soft tissue thickness. There are a few possible explanations for this:

1. Of the tissues measured (muscle, adipose, total), adipose tissues are closest to the surface of the skin and therefore closer to the ultrasound probe. Ultrasound waves are attenuated as they pass through tissues, with greater attenuation occurring at deeper imaging depths (Hoskins, Martin, & Thrush, 2019). The result of this increase in attenuation is a reduction in image quality at deeper depths (Thoirs, K., 2012). Muscle is deeper than subcutaneous adipose tissue and is therefore likely subject to reduced image quality compared to the adipose tissues. The reduced image quality could explain the lower reliability for muscle thickness measurements compared to adipose. The same rationale can be applied to measurements of total soft tissue thickness and can likely explain why reliability is lower for total thickness compared to adipose thickness, as well as why the reliability between muscle and total thicknesses is similar.

2. Adipose tissues are likely less sensitive to participant movement than muscle and total soft tissues are. Ultrasound measurements of muscle thickness have been shown to change with muscle contraction across a range of muscles in the human body, particularly at low levels of muscle activation (Hodges, Pengel, Herbert, & Gandevia, 2003; McMeeken, Beith, Newham, Milligan, & Critchley, 2004). While participants were instructed to remain as still and relaxed as possible during imaging trials, there was still some movement and low levels of muscle

activation may have occurred. The slight movement and potential low levels of muscle activation may have resulted in small changes in muscle thickness between trials, resulting in the lower reliability of muscle thickness measurements compared to adipose. Since muscle thickness makes up on average 60% of total soft tissue thickness while adipose makes up 35%, differences in thickness measurements of muscle will have a greater influence on measurements of total soft tissue thickness, and therefore have greater impact on the reliability of total thickness measurements as well.

3. Finally, as stated above, on average, muscle contributes more to total soft tissue thickness than adipose tissue does. Due to the greater average contribution of muscle to total soft tissues, measurements of muscle thickness (and their corresponding reliability) will have a greater influence on the overall reliability of total soft tissue thickness measurements.

Reliability of both muscle and total soft tissue thickness measurements was worse at A1 and P1 measurement locations compared to all other locations. There are a few possible explanations for this:

1. There are potential protocol-related explanations for the lower reliability at A1 and P1 locations. The cut-out of the table which allowed for ultrasound imaging of the side of the femur that would impact the ground during a fall event made manipulation of the ultrasound probe awkward at A1 and P1 locations. Accordingly, consistency with probe positioning and orientation was more challenging at these locations and therefore may have contributed to the reduced reliability seen. In addition to this, the investigator had to occasionally ask participants to change their positioning on the table to successfully obtain ultrasound images at A1 and P1 locations. This change in participant positioning could have resulted in movement of the skin marking relative to the underlying femur, leading to small differences in thickness measurements between trials, and therefore contributing to the lower reliability.

2. There are also potential anatomical explanations for why reliability was worse at A1 and P1 locations. Since the measurement grid was standardized and not scaled to individual participant anthropometrics, the exact location of the skin markings relative to the underlying femur can vary between participants. Specific to the A1 and P1 locations, in some participants, these locations were directly over the hip joint. Due to the definitions of how soft tissue thicknesses were measured, a bony surface in the middle of the image was required to measure against. As a result, the investigator had to use their best judgement when maneuvering the ultrasound probe to obtain the image. Depending on which way the

56

investigator moved the probe, the underlying bony surface could either become the head of the femur or the acetabulum of the pelvis, which would influence the thickness measurements in any given trial. In addition to this, the need to maneuver the ultrasound probe at these locations increased the likelihood that probe positioning and orientation were not consistent between trials. Taken together, these factors likely contributed to the lower reliability seen at A1 and P1 locations.

As a reminder, the intra-rater reliability of the protocol was assessed in this thesis. More specifically, the intra-rater reliability of the probe repositioning, image acquisition, and image analysis was investigated. In addition to the potential sources of variability discussed above, there are a few more potential sources of error worth discussing. Potential sources of error related to probe repositioning include maneuvering the probe within the confines of the table, the ability to consistently place the probe in the same spot on the surface of the skin, and ensuring that the probe orientation was consistent between trials (i.e always oriented perpendicular to the long axis of the femur). Potential sources of error related to image acquisition include potential low levels of muscle contraction during trials, participant movement between trials, and the amount of time spent in the side-lying position during imaging. Since soft tissue thickness was measured from underneath participants, there was the potential for gravitational effects to increase soft tissue thickness over time. To help mitigate the influence of time spent in the side-lying position on measurements of soft tissue thickness, the order locations were imaged in was randomized. Finally, potential sources of error related to image analysis include the ability to consistently select the skin surface pixel that is in the middle of the ultrasound image and consistently select the pixel corresponding to the outer edge of the femur, outer edge of the muscle fascia, and inner edge of the skin surface. To explore the intra-rater reliability of the image analysis, thicknesses of muscle, adipose and total soft tissues at point L2 were measured on a second day. The difference between the original and re-measured values ranged between 0 to 3.65 mm, with the average difference in muscle, adipose, and total thicknesses being 0.57 (0.85) mm, 0.7 (0.85), and 0.25 (0.31) mm respectively. The re-measured values were, on average, within 2.0 (13.1) % of the original values. Accordingly, I have a high level of confidence in the reliability of my image analysis measures.

The ICC values in this thesis are generally similar to results published in other ultrasound reliability studies. Thoirs and English (2009) investigated the intra-rater reliability of ultrasound measured muscle thickness over a variety of sites on the human body, and the influence of body position on the

reliability results. The authors reported ICCs of 0.89 over the anterior thigh and 0.7 over the posterior thigh for measures taken in a standing position. For measures taken in a recumbent position, ICCs were 0.9 over the anterior thigh and 0.71 over the posterior thigh. The average ICC value for muscle (ICC = 0.847) in this thesis is similar to the ICC over the anterior thigh and greater than the ICC over the posterior thigh in the work done by Thoirs and English (2009). The difference in ICCs between the studies could be explained by differences in participant positioning (side-lying vs standing, supine, or prone) as well as differences in the specific measurement location over the thigh.

Mendis et al. (2010) investigated the intra-rater reliability of ultrasound measured thickness of the following anterior hip muscles from both the left and right leg of human volunteers: iliopsoas, sartorius, and rectus femoris. They found ICCs ranging from 0.81 – 0.89. While different muscles were measured in this thesis compared to their study, comparisons can still be made. The average ICC for muscle thickness (ICC = 0.847) in this thesis falls within the range of muscle ICCs reported by Mendis and colleagues (2010), while the range of muscle ICCs (ICC = 0.486 – 0.979) falls both above and below the range of ICC values reported by Mendis and colleagues (2010). Once again, differences in reported ICCs between the studies can be explained by protocol related differences, with measurements taken at different locations over the thigh (anterior vs lateral) and with participants in different positions (supine vs side-lying) between the studies.

Lanza et al. (2022) investigated reliability of ultrasound measured gluteus medius and tensor fascia latea muscle thickness and the corresponding thickness of the subcutaneous tissues overlying these muscles. They found ICCs of 0.9 for gluteus medius muscle thickness, 0.98 for tensor fascia latae muscle thickness, 0.98 for subcutaneous tissue thickness over the gluteus medius, and 0.96 for subcutaneous tissue thickness over the tensor fascia latae. The average adipose ICC across locations of 0.955 in this thesis is similar to the values of 0.98 over the gluteus medius muscle and 0.96 over the tensor fascia latae muscle reported by Lanza et al. (2022). While our average ICC value of 0.847 for muscle thickness across locations was approximately 0.05 points lower than the gluteus medius muscle and 0.13 points lower than tensor fascia latae muscle ICCs reported by Lanza and colleagues (2022), the trend of muscle ICCs being lower than adipose ICCs was the same in both studies.

Betz et al. (2021) reported intra-rater reliability for measurements of subcutaneous adipose tissue and vastis lateralis muscle thickness in healthy young adults. They reported muscle ICCs = 0.928 – 0.946 and adipose ICCs = 0.992 – 0.994, which directly aligns with our trend of higher ICCs for adipose thickness compared to muscle thickness. Our reported adipose ICCs = 0.906 – 0.996 are directly

aligned with the values reported by Betz and colleagues (2021). However, our reported muscle ICCs (ICC = 0.486 – 0.979) are on average lower than those reported by Betz (2021). One reason for this is our poor and moderate reliability for muscle thickness measurements at A1 and P1 locations. If we exclude these locations, our average muscle ICC = 0.91 (ICC range = 0.853 – 0.976) is more aligned with their results.

Levine et al. (2015) reported ICCs for ultrasound measured TSTT across different hip positions of ICC > 0.98. Across conditions, the ICC for TST in this thesis was on average 0.867, which is lower than that reported by Levine et al. (2015). However, our ICCs ranged between 0.804 – 0.997 for total thickness, with all but two measurement locations having ICCs ≥ 0.945, which aligns with the values reported by Levine and colleagues (2015). The difference in reliability can be explained through protocol differences. We measured soft tissue thickness over 12 different locations while Levine et al. (2015) only measured over the GT. The lower ICCs at A1 and P1 locations contribute to the lower average ICC for TST in this thesis. Looking solely at the ICCs over the GT in this thesis for muscle, adipose, and total soft tissue thickness, values were 0.98, 0.99, and 0.99 respectively, which aligns with the results published by Levine and colleagues (2015). Participants in this thesis were in a side-lying position with hips and knees straight during imaging while participants in the Levine et al. (2015) study were in a standing position with differing amounts of hip flexion/extension and abduction/adduction. Participant positioning can influence reliability results, with standing and side-lying measurements having better reliability than supine measurements (Lafleur, Benoit, 2016) .

This thesis also measured soft tissue thickness across 12 locations, with two of the locations (A1 and P1) having poor or moderate ICCs for muscle and total soft tissues. The lower ICCs at these two locations contribute to the lower average ICC values for muscle and total soft tissue thickness reported in this thesis. Excluding ICCs for muscle and total thickness at A1 and P1 locations A1, our ICCs were no lower than 0.854 with at least 50% of the locations having ICCs > 0.9. These values align well with the other reported ICCs for ultrasound measured soft tissue thickness in the literature (Betz et al., 2021; Lanza et al., 2022; Levine et al., 2015; Mendis et al., 2010; Thoirs, Kerry & English, 2009).

3.3.2 Soft Tissue Thickness and Composition

To my knowledge there are no studies on muscle thickness over the lateral proximal femur, making direct comparisons between our values and those in the literature challenging. However, to show that my reported values are reasonable, comparisons will be made where possible. Across locations, our

muscle thickness values ranged between 8.34 (6.43) – 52.27 (11.27) mm and were on average 36.3 (18) mm. Arts and colleagues (2010) reported quadriceps femoris muscle thickness ranging between 35.7 (7.2) – 41.6 (10.2) mm. While the range of muscle thicknesses reported in this thesis falls both above and below the values reported by Arts et al. (2010), there are two large differences in the methodologies between the studies that likely accounts for the differences in reported muscle thickness values. The first being that muscle thickness measurements were taken at different locations: Arts and colleagues (2010) measured muscle thickness at one location halfway along the line between the ASIS and the patella with participants lying supine while we measured muscle thickness over 12 locations on the lateral proximal femur with participants side-lying. Therefore, the specific muscles included in the thickness measurements between studies differ. Additionally, gravitational effects are likely to influence the thickness results differently between the studies. The supine position employed by Arts et al. (2010) is more likely to result in gravity reducing the thickness of the soft tissues while the side-lying position we used is more likely to result in gravity increasing the thickness of the soft tissues.

Our values of adipose thickness were generally comparable to values reported in the literature. Across locations, our adipose thickness values ranged between 10.28 (6.66) – 30.02 (16.05) mm and were on average 19.8 (12.9) mm. Anvery and colleagues (2022) used high resolution ultrasound to measure subcutaneous adipose tissue thickness in males and females aged 20 – 70 years. Over the posterior thigh, they reported adipose thicknesses of 8.6 (5.8) – 14.1 (5.7) mm and over the lateral thigh, they reported thickness of 11.9 (6.3) – 24.5 (15.6) mm. While the upper end of our adipose thickness measurements was greater than those reported by Anvery (2022), the differences can be explained by differences in the methodology between the two studies. Participants were in different positions when ultrasound measurements were being taken (side-lying vs standing). The side-lying position used in this thesis subjected the soft tissues to greater gravitational effects than the standing position used by Anvery and colleagues (2022). These gravitational effects likely increased our thickness measurements compared to those reported by Anvery and colleagues. The exact locations being measured also differed between the studies, with 12 locations over the proximal lateral femur imaged in this thesis, and one location over the posterior thigh and one location over the lateral thigh imaged in the work done by Anvery and colleagues (2022). The implication of these different locations is that the adipose included in the thickness measurements between studies comes from different locations and can therefore contribute to the differences in thicknesses seen. Finally, Anvery et al. (2022) had participants ranging from 20 – 70 years of age while participants in this thesis were between 20 – 25

years of age. The age difference between the two studies may also contribute to the differences in adipose thickness measurement.

Our values of total thickness over the GT were generally comparable to values reported in the literature. Total soft tissue thickness values over the GT in this thesis ranged between 13.26 – 86.6 mm and were on average 31.4 (16.7) mm. Previous measurements of ultrasound measured soft tissue thickness over the GT ranged between 11.4 – 122.1 mm, with average reported values ranging between 18.1 – 55.7 mm (Choi et al., 2015; Lafleur, Benoit, 2016; Lafleur, Benoit R. et al., 2021; Levine et al., 2015; Lim & Choi, 2021; Maitland et al., 1993; Minns et al., 2007; Robinovitch et al., 1991).

Our values of male and female total thickness over the GT also align with values reported in the literature. While five studies measured TSTT using ultrasound in both male and female participants (Lafleur, Benoit, 2016; Lafleur, Benoit R. et al., 2021; Levine et al., 2015; Lim & Choi, 2021; Pretty, Steven P. et al., 2021b; Pretty, Steven P. et al., 2021a; Robinovitch et al., 1991), only four studies report TSTT for males and females separately (Levine et al., 2015; Pretty, Steven P. et al., 2021b; Pretty, Steven P. et al., 2021a; Robinovitch et al., 1991). Levine and colleagues (2015) report that the average male TSTT is 22.8 (9.7) mm, Robinovitch and colleagues (1991) report male TSTT being on average 17.1 mm, and Pretty and colleagues (2021b; 2021a) report low BMI male TSTT being 24 (4) mm. We found that the average total soft tissue thickness over the GT for males was 22.7 (10.7) mm. This is directly aligned with results published by Levine et al. (2015) and Pretty et al. (2021b; 2021a), and is slightly larger than the results published by Robinovitch and colleagues (1991). The difference between results published in this thesis and those published by Robinovitch (1991) is likely the different position participants were in during ultrasound imaging (standing in the Robinovitch study, side-lying in this thesis). Ten studies measured TSTT using ultrasound in females (Choi et al., 2015; Lafleur, Benoit, 2016; Lafleur, Benoit R. et al., 2021; Levine et al., 2015; Lim & Choi, 2021; Maitland et al., 1993; Minns et al., 2007; Pretty, Steven P. et al., 2021b; Pretty, Steven P. et al., 2021a; Robinovitch et al., 1991). When both males and females participated in the study, only four studies reported female specific TSTT (Levine et al., 2015; Pretty, Steven P. et al., 2021b; Pretty, Steven P. et al., 2021a; Robinovitch et al., 1991). Across these studies, average TSTT ranged between 18.1 mm for older adult females who experienced a hip fracture (Minns et al., 2007) to 42 (3) mm in healthy young adult females (Pretty, Steven P. et al., 2021b; Pretty, Steven P. et al., 2021a). Other reported female TSTT values were 32.1 (7.2) mm (Choi et al., 2015), 33.3 (6.6) mm (Levine et al.,

2015), and 35 mm (Robinovitch et al., 1991). We found that average total soft tissue thickness over the GT was 39.1 (17.3) mm for healthy young adult females. Our female TSTT is similar to that of the afore mentioned reported female TSTT values in the literature. Differences between female TSTT in this thesis and other published studies are likely due to differences in participant positioning. Participants were in a side-lying position with measurements taken from the side of the body that would impact the ground in this thesis, while other studies used standing or side-lying (measured from above) positions. Gravitational effects would likely pull on the soft tissues as measured in this thesis, creating the slightly greater TSTT seen compared to most of the other published literature.

This thesis provides important insights on soft tissue thickness differences across sex. On average total and adipose thicknesses were 13.6% and 46.4% greater for females compared to males while muscle thickness was on average 8.6 % greater for males compared to females. These sex related differences between tissue types are not surprising as females are known to have greater adipose, greater total soft tissues over the hip, and less muscle than males (Bredella, 2017; Levine et al., 2015; Ley et al., 1992; Schorr et al., 2018). In addition to this, females are also known to have more of a gynoid distribution of adipose tissues while males have more of an android distribution of adipose tissues (Bredella, 2017; Ley et al., 1992; Schorr et al., 2018), meaning that females carry more adipose tissues over the hip and thigh region while males carry more adipose tissues over the abdominal region.

These sex related differences have potential implications for impact dynamics during lateral falls. Lower soft tissue thickness should lead to less force attenuation during impact from a sideways fall as Robinovitch (1995) found that for every 1 mm increase in TSTT, there is a corresponding 71 N decrease in predicted impact forces. Applying this to our total soft tissue thickness data, females would experience, on average, 609.8 N greater reduction in impact forces compared to males. This finding aligns with epidemiological data that shows TSTT is protective against hip fracture in females but not males (Dufour et al., 2012; Nasiri & Luo, 2016). This may be because there are less total soft tissues over the proximal femur in males compared to females.

What is less clear in the literature, is how much of that reduction in predicted peak impact forces is due to muscle and how much is due to adipose thickness. Due to the 32.8% difference in percent contribution between muscle and adipose to total soft tissue thickness over the GT (61.5% adipose, 28.7% muscle), we can postulate that each tissue will differentially contribute to force attenuation during an impact. However, the tissue-specific thicknesses and percent contribution of each tissue to

total thickness differs across locations. For example, at A3 the percent contribution of muscle was 75.3% and adipose was 21.4%. In contrast, L3 was 45.7% muscle and 48.9% adipose while P3 was 46.9% muscle and 48.7% adipose. Accordingly, the differences in muscle and adipose thicknesses over the proximal femur have potential implications for impact dynamics during lateral falls. From a deformation perspective, it is reasonable to expect that muscle and adipose tissues will differentially compress during impact based solely on the differences in their thicknesses at a given location (i.e. the tissue with the larger thickness has the capacity to deform more during impact compared to the tissue with the lower thickness). When tissue-specific thicknesses are similar (such as at the example L3 and P3 locations above), it is still reasonable to expect that individual tissues would differentially contribute to energy absorption during lateral falls based on differences in tissue-specific mechanical properties. For example, studies have found that the stiffness of muscle is greater than that of adipose tissue (Chakouch, Charleux, & Bensamoun, 2015; Debernard, Leclerc, Robert, Charleux, & Bensamoun, 2013). Both Debernard et al. (2013) and Chakouch et al. (2015) used magnetic resonance elastography to quantify the elastic shear modulus of muscles in the human thigh. In addition to muscle shear modulus, the authors also measured shear modulus for subcutaneous adipose tissues. Debernard et al. (2013) reported shear moduli ranging between 3.67 – 6.89 kPa for muscles at rest, 11.29 kPa for vastus medialis at 20% MVC, and 1.61 kPa for subcutaneous adipose tissues. Chakouch et al. (2015) reported similar values for shear modulus of muscle and a higher shear modulus for subcutaneous adipose tissues compared to those reported by Debernard et al. (2013). Specifically, Chakouch et al. (2015) reported shear moduli ranging between 3.74 – 6.15 kPa for thigh muscles at rest and a shear modulus of 3.04 kPa for subcutaneous adipose tissues. The shear modulus for adipose tissues was significantly lower than that of the muscle tissues in both studies. These tissue-specific differences in shear modulus support the theory that muscle and adipose tissues may differentially contribute to force attenuation during sideways falls, and highlights the importance of considering muscle and adipose tissues separately in mechanical models of hip fracture.

Returning to our discussion on sex-based differences, males have greater muscle thickness and less adipose thickness than females. In addition to the total thickness differences discussed above, and the differences in the mechanical properties of muscle and adipose tissues, the increased contribution of muscle in males may further explain the non-significant effects of soft tissue thickness on hip fracture risk in males.

3.3.3 Limitations

There are several limitations associated with this work that need to be acknowledged. First, the investigator measuring soft tissue thickness with the ultrasound machine was not an expert sonographer. However, the investigator has completed extensive training on the use of ultrasound for measuring soft tissue thickness over the lateral proximal femur. The investigator completed over 20 hours of training on proper use of ultrasound and has collected ultrasound measured TSTT as a second investigator in a previous research study (Lafleur, Benoit, 2016).

Second, the grid used to mark the imaging locations on participants was a standardized grid with absolute dimensions and was not scaled to individual participant anthropometrics. Accordingly, the exact locations over the femur being imaged may have differed slightly between participants based on their thigh and pelvis geometry. This limitation was addressed by taking measurements of thigh circumference, hip circumference, and distances between point L1 and the ASIS as well as L1 and the iliac crest to provide insights into the location of the grid relative to a few anatomical landmarks (aside from just the GT). All measured distances were similar between males and females (Table 7). Another justification for the use of a standardized measurement grid is that current wearable devices for hip fracture prevention (i.e. hip protectors) are not person-specific. To better understand why these devices are effective for some individuals and not others, we need to better understand the distribution of the soft tissues across a standardized area that these devices cover before considering person-specific tissue composition and customized protective devices. Finally, the standardized grid used in this thesis aligns with the CSA Z325:20 standard for testing hip protectors. By aligning the grid with the CSA standard, we have provided information on the distribution of the soft tissues under the locations where hip protectors are tested.

Third, while participants were instructed to remain as relaxed as possible, they did not remain perfectly still throughout the entire data collection session. Any movement of the participant on the table had the potential to move the skin marking relative to the underlying femur, thereby having the potential to influence reliability by changing the exact location being imaged. In addition to this, movement generates muscle contraction, which can alter muscle thickness (Hodges et al., 2003; McMeeken et al., 2004). To help mitigate the influence of muscle contraction on thickness measurements, images were only taken once participants relaxed their muscles again (as seen visually on the real-time ultrasound image).

Fourth, there were no older adults recruited for this study. While this thesis provides an understanding of the composition and distribution of soft tissues over the lateral proximal femur in young adults and shows that the ultrasound protocol used is generally reliable in young adults, it may not be generalizable to the older adult population (which is at a greater risk of experiencing a fall-related hip fracture (Jean et al., 2013)).

Fifth, pressure of the ultrasound transducer against the skin surface was not quantified. Differences in pressure between images were possible and could affect the thickness measurements by compressing the underlying soft tissues. Whenever possible, the investigator maintained a clear visual of the ultrasound gel overtop of the skin surface to mitigate the potential for compression of the soft tissues by the ultrasound probe.

Finally, the cut-out on the table which allowed for imaging of the side of the femur that would impact the femur resulted in soft tissue bulging, particularly over the posterolateral measurement locations. This may have distorted soft tissue thickness measurements in this area, and unintentionally provided slightly larger thickness measurements over the posterolateral locations.

.

Chapter 4
Thesis Synthesis and Conclusions

4.1 Novel Contributions and Impact

This thesis is the first to use b-mode ultrasound to measure the thickness of muscle, adipose, and total soft tissues over multiple locations over the proximal femur in a simulated sideways fall configuration. Several novel findings come from the results of this thesis:

Firstly, soft tissue thickness and composition can be reliably measured across the lateral proximal femur, except for locations A1 and P1, which are located 6 cm anterior/posterior and 6 cm proximal to the GT.

Secondly, tissue specific as well as bulk tissue thicknesses can be reliably measured in a simulated sideways fall configuration. By measuring soft tissue thickness in this clinically relevant configuration, we are the first to provide data on the thickness and distribution of muscle, adipose, and total soft tissues over the lateral proximal femur in a relevant fall orientation (i.e. in the orientation they would be in during impact from a sideways fall onto the hip).

Thirdly, by measuring the thickness of muscle and adipose tissues in addition to total soft tissues, we are the first to provide data on the differing contributions of muscle and adipose tissues to bulk soft tissue thickness. We have shown that muscle and adipose tissues differentially contribute to bulk soft tissue thickness across locations over the lateral proximal femur. By demonstrating that individual tissues differentially contribute to bulk soft tissue thickness, we have highlighted the need for considering tissue-specific thicknesses in future research regarding hip fracture risk, the design of intervention techniques, and mechanical models of hip fracture.

Fourthly, by measuring soft tissue thickness at 12 locations over the lateral proximal femur, we have expanded on previous research which only considered the thickness of the tissues lying directly over the GT. We have provided crucial information regarding the distribution of muscle, adipose, and total soft tissue thickness over the lateral proximal femur. The results of this thesis can be used in future research regarding the role of soft tissues during an impact.

4.2 Future Research

While we have shown that soft tissue thickness and composition vary across the lateral proximal femur, there is more research to be done with regards to the relationship between soft tissues and hip fracture. Research is needed to determine the differential force attenuation provided by muscle and adipose tissues, and how differing contributions of muscle and adipose may be relevant to hip fracture risk. Additionally, a comparison of soft tissue thickness and composition between hip fracture and non-fracture populations should be performed. Doing so would provide crucial insights into the relationship between soft tissue thickness and hip fracture through investigation of differences in the individual soft tissue thicknesses and their distribution over the proximal femur.

Future research should also include expanding the protocol we used to an older adult population. There are two reasons for this: 1) We have shown that ultrasound can be used to reliably measure individual tissue thicknesses in a young adult population, however, the reliability of our protocol still needs to be assessed in the older adult population.; and 2) Our soft tissue thickness results may not be generalizable to the older adult population, which is the population at greater risk of experiencing a hip fracture (Jean et al., 2013). Work assessing the composition of soft tissues in this population is crucial to further our understanding of the relationship between soft tissues and impact dynamics.

Finally, future research should explore the inter-rater reliability of the protocol and investigate which measurement location (or locations), and the corresponding soft tissues at that location(s), have the best relationship with hip fracture risk.

4.3 Conclusions

This thesis is the first to demonstrate that b-mode ultrasound can be used to reliably measure muscle, adipose, and total soft tissue thickness over multiple locations on the proximal femur in a simulated sideways fall configuration. Our results provide novel insights into sex and location-based differences in tissue-specific thicknesses over the proximal femur, with both sex and location influencing measures of soft tissue thickness. We found that males have greater muscle, less adipose, and less total soft tissues than females. These sex-based differences provide insights into potential explanations for the differential efficacy of TSTT in reducing hip fracture risk between males and females. We found that muscle thickness was greatest over the anterolateral femur and lowest over the lateral femur; adipose thickness was greatest over the posterolateral femur and lowest over the anterolateral femur; and total soft tissue thickness was greatest over both the anterolateral and

posterolateral femur, and lowest over the lateral femur. The location-based differences across tissue types highlight the importance of considering individual tissue thicknesses surrounding the GT into future work regarding the relationship between soft tissues and hip fracture. Finally, the differential contributions of muscle and adipose tissues to bulk tissue thickness across measurement locations highlights the importance of considering tissue-specific thicknesses into mechanical models of hip fracture.

List of References

Adachi, J. D., Ioannidis, G., Berger, C., Joseph, L., Papaioannou, A., Pickard, L., . . . Prior, J. C. (2001). The influence of osteoporotic fractures on health-related quality of life in community-dwelling men and women across canada. *Osteoporosis International, 12*(11), 903-908.

Alswat, K. A. (2017). Gender disparities in osteoporosis. *Journal of Clinical Medicine Research, 9*(5), 382.

Anvery, N., Wan, H. T., Dirr, M. A., Christensen, R. E., Weil, A., Raja, S., . . . Poon, E. (2022). Utility of high-resolution ultrasound in measuring subcutaneous fat thickness. *Lasers in Surgery and Medicine, 54*(9), 1189-1197.

Arts, I. M., Pillen, S., Schelhaas, H. J., Overeem, S., & Zwarts, M. J. (2010). Normal values for quantitative muscle ultrasonography in adults. *Muscle & Nerve: Official Journal of the American Association of Electrodiagnostic Medicine, 41*(1), 32-41.

Bachmann, K. N., Fazeli, P. K., Lawson, E. A., Russell, B. M., Riccio, A. D., Meenaghan, E., . . . Miller, K. K. (2014). Comparison of hip geometry, strength, and estimated fracture risk in women with anorexia nervosa and overweight/obese women. *The Journal of Clinical Endocrinology and Metabolism, 99*(12), 4664-4673. doi:10.1210/jc.2014-2104

Berger, A. (2002). How does it work?: Bone mineral density scans. *BMJ: British Medical Journal, 325*(7362), 484.

Betz, T. M., Wehrstein, M., Preisner, F., Bendszus, M., & Friedmann-Bette, B. (2021). Reliability and validity of a standardized ultrasound examination protocol to quantify vastus lateralis muscle. *Journal of Rehabilitation Medicine, 53*(7)

Bhan, S., Levine, I., & Laing, A. C. (2013). The influence of body mass index and gender on the impact attenuation properties of flooring systems. *Journal of Applied Biomechanics, 29*(6), 731-739.

Bhattacharya, P., Altai, Z., Qasim, M., & Viceconti, M. (2019). A multiscale model to predict current absolute risk of femoral fracture in a postmenopausal population. *Biomechanics and Modeling in Mechanobiology, 18*(2), 301-318. doi:10.1007/s10237-018-1081-0

Black, D., Vora, J., Hayward, M., & Marks, R. (1988). Measurement of subcutaneous fat thickness with high frequency pulsed ultrasound: Comparisons with a caliper and a radiographic technique. *Clinical Physics and Physiological Measurement, 9*(1), 57.

Bouxsein, M. L., Szulc, P., Munoz, F., Thrall, E., Sornay-Rendu, E., & Delmas, P. D. (2007). Contribution of trochanteric soft tissues to fall force estimates, the factor of risk, and prediction of hip fracture risk. *Journal of Bone and Mineral Research : The Official Journal of the American Society for Bone and Mineral Research, 22*(6), 825-831. doi:10.1359/jbmr.070309

Bredella, M. A. (2017). Sex differences in body composition. *Sex and Gender Factors Affecting Metabolic Homeostasis, Diabetes and Obesity, , 9-27.*

Chakouch, M. K., Charleux, F., & Bensamoun, S. F. (2015). Quantifying the elastic property of nine thigh muscles using magnetic resonance elastography. *PLoS One, 10*(9), e0138873.

Chan, V., & Perlas, A. (2011). Basics of ultrasound imaging. *Atlas of ultrasound-guided procedures in interventional pain management* (pp. 13-19) Springer.

Chevalley, T., Guilley, E., Herrmann, F. R., Hoffmeyer, P., & Rizzoli, R. (2007). Incidence of hip fracture over a 10-year period (1991–2000): Reversal of a secular trend.*40*(5), 1284-1289.

Choi, W. J., Russell, C. M., Tsai, C. M., Arzanpour, S., & Robinovitch, S. N. (2015). Age-related changes in dynamic compressive properties of trochanteric soft tissues over the hip. *Journal of Biomechanics, 48*(4), 695-700. doi:10.1016/j.jbiomech.2014.12.026

Cummings, S. R., & Nevitt, M. C. (1989). A hypothesis: The causes of hip fractures. *Journal of Gerontology, 44*(5), M107-M111.

De Laet, C., Kanis, J. A., Oden, A., Johanson, H., Johnell, O., Delmas, P., . . . Tenenhouse, A. (2005). Body mass index as a predictor of fracture risk: A meta-analysis. *Osteoporosis International : A Journal Established as Result of Cooperation between the European Foundation for Osteoporosis and the National Osteoporosis Foundation of the USA, 16*(11), 1330-1338. doi:10.1007/s00198-005-1863-y

Debernard, L., Leclerc, G. E., Robert, L., Charleux, F., & Bensamoun, S. F. (2013). In vivo characterization of the muscle viscoelasticity in passive and active conditions using multifrequency MR elastography. *Journal of Musculoskeletal Research, 16*(02), 1350008.

Dufour, A. B., Roberts, B., Broe, K. E., Kiel, D. P., Bouxsein, M. L., & Hannan, M. T. (2012). The factor-of-risk biomechanical approach predicts hip fracture in men and women: The framingham study. *Osteoporosis International : A Journal Established as Result of Cooperation between the*

European Foundation for Osteoporosis and the National Osteoporosis Foundation of the USA, 23(2), 513-520. doi:10.1007/s00198-011-1569-2

Dufour, A. B., Roberts, B., Broe, K. E., Kiel, D. P., Bouxsein, M. L., & Hannan, M. T. (2019). Correction to: The factor-of-risk biomechanical approach predicts hip fracture in men and women: The framingham study. *Osteoporosis International, 30*(9), 1897.

Empana, J., Dargent-Molina, P., Bréart, G., & EPIDOS Group. (2004). Effect of hip fracture on mortality in elderly women: The EPIDOS prospective study. *Journal of the American Geriatrics Society, 52*(5), 685-690.

Etheridge, B. S., Beason, D. P., Lopez, R. R., Alonso, J. E., McGwin, G., & Eberhardt, A. W. (2005). Effects of trochanteric soft tissues and bone density on fracture of the female pelvis in experimental side impacts. *Annals of Biomedical Engineering, 33*(2), 248-254.

Fleps, I., Enns-Bray, W., Guy, P., Ferguson, S. J., Cripton, P. A., & Helgason, B. (2018). On the internal reaction forces, energy absorption, and fracture in the hip during simulated sideways fall impact. *PLoS One, 13*(8), e0200952.

Fleps, I., Guy, P., Ferguson, S. J., Cripton, P. A., & Helgason, B. (2019). Explicit finite element models accurately predict subject-specific and velocity-dependent kinetics of sideways fall impact. *Journal of Bone and Mineral Research, 34*(10), 1837-1850.

Galliker, E. S., Laing, A. C., Ferguson, S. J., Helgason, B., & Fleps, I. (2022). The influence of fall direction and hip protector on fracture risk: FE model predictions driven by experimental data. *Annals of Biomedical Engineering, 50*(3), 278-290.

Gregory, J. S., & Aspden, R. M. (2008). Femoral geometry as a risk factor for osteoporotic hip fracture in men and women. *Medical Engineering & Physics, 30*(10), 1275-1286.

Hansen, W. E., & Kehrer, H. (1987). Assessment of cutaneous fat and body fat by ultrasound. *Klinische Wochenschrift, 65*(9), 407-410.

Hayes, W. C., Myers, E. R., Robinovitch, S. N., Van Den Kroonenberg, A., Courtney, A. C., & McMahon, T. A. (1996). Etiology and prevention of age-related hip fractures. *Bone, 18*(1 Suppl), 77S-86S. doi:8756-3282(95)00383-5 [pii]

Hida, T., Ando, K., Kobayashi, K., Ito, K., Tsushima, M., Kobayakawa, T., . . . Ota, K. (2018). Ultrasound measurement of thigh muscle thickness for assessment of sarcopenia. *Nagoya Journal of Medical Science, 80*(4), 519.

Hodges, P. W., Pengel, L., Herbert, R. D., & Gandevia, S. (2003). Measurement of muscle contraction with ultrasound imaging. *Muscle & Nerve: Official Journal of the American Association of Electrodiagnostic Medicine, 27*(6), 682-692.

Hoskins, P. R., Martin, K., & Thrush, A. (2019). *Diagnostic ultrasound: Physics and equipment* (Third ed.) Cambridge University Press.

Jean, S., O'Donnell, S., Lagacé, C., Walsh, P., Bancej, C., Brown, J. P., . . . Leslie, W. D. (2013). Trends in hip fracture rates in canada: An age-period-cohort analysis. *Journal of Bone and Mineral Research, 28*(6), 1283-1289.

Johansson, H., Kanis, J. A., Odén, A., Johnell, O., & McCloskey, E. (2009). BMD, clinical risk

    factors and their combination for hip fracture prevention. *Osteoporosis International, 20*(10),

    1675-1682.

Johansson, H., Kanis, J. A., Odén, A., McCloskey, E., Chapurlat, R. D., Christiansen, C., . . .

    Fujiwara, S. (2014). A meta-analysis of the association of fracture risk and body mass index in

    women. *Journal of Bone and Mineral Research, 29*(1), 223-233.

Kanis, J. A., Borgstrom, F., De Laet, C., Johansson, H., Johnell, O., Jonsson, B., . . . Khaltaev, N.

    (2005). Assessment of fracture risk. *Osteoporosis International, 16*(6), 581-589.

Koo, T. K., & Li, M. Y. (2016). A guideline of selecting and reporting intraclass correlation

    coefficients for reliability research. *Journal of Chiropractic Medicine, 15*(2), 155-163.

    doi:10.1016/j.jcm.2016.02.012 [doi]

Korall, A. M., Feldman, F., Yang, Y., Cameron, I. D., Leung, P., Sims-Gould, J., & Robinovitch, S.

    N. (2019). Effectiveness of hip protectors to reduce risk for hip fracture from falls in long-term

    care. *Journal of the American Medical Directors Association, 20*(11), 1397-1403. e1.

Kossoff, G. (2000). Basic physics and imaging characteristics of ultrasound. *World Journal of*

    Surgery, 24(2), 134-142.

Lafleur, B. (2016). *Factors influencing measures of trochanteric soft tissue thickness*

    (Dissertation/Thesis).

Lafleur, B. R., Tondat, A. M., Pretty, S. P., Mourtzakis, M., & Laing, A. C. (2021). The effects of

    body position on trochanteric soft tissue Thickness—Implications for predictions of impact force

    and hip fracture risk during lateral falls. *Journal of Applied Biomechanics, 37*(6), 556-564.

Laing, A. C., & Robinovitch, S. N. (2008). Effect of soft shell hip protectors on pressure distribution

    to the hip during sideways falls. *Osteoporosis International, 19*(7), 1067-1075.

Laing, A. C., & Robinovitch, S. N. (2009). Low stiffness floors can attenuate fall-related femoral

    impact forces by up to 50% without substantially impairing balance in older women. *Accident

    Analysis & Prevention, 41*(3), 642-650.

Lanza, M. B., Rock, K., Marchese, V., Gray, V. L., & Addison, O. (2022). Ultrasound measures of

    muscle thickness and subcutaneous tissue from the hip abductors: Inter-and intra-rater reliability.

    Musculoskeletal Science and Practice, 62, 102612.

Laskey, M. A. (1996). Dual-energy X-ray absorptiometry and body composition. *Nutrition, 12*(1), 45-

    51.

Leahy, S., Toomey, C., McCreesh, K., O'Neill, C., & Jakeman, P. (2012). Ultrasound measurement

    of subcutaneous adipose tissue thickness accurately predicts total and segmental body fat of

    young adults. *Ultrasound in Medicine & Biology, 38*(1), 28-34.

Leslie, W. D., O'Donnell, S., Jean, S., Lagacé, C., Walsh, P., Bancej, C., . . . Osteoporosis

    Surveillance Expert Working Group. (2009). Trends in hip fracture rates in canada. *Jama,

    302*(8), 883-889.

Levine, I. C., Minty, L. E., & Laing, A. C. (2015). Factors that influence soft tissue thickness over the greater trochanter: Application to understanding hip fractures. *Clinical Anatomy (New York, N.Y.), 28*(2), 253-261. doi:10.1002/ca.22499

Ley, C. J., Lees, B., & Stevenson, J. C. (1992). Sex-and menopause-associated changes in body-fat distribution.*55*(5), 950-954.

Lim, K. T., & Choi, W. J. (2021). The effect of the hip impact configuration on the energy absorption provided by the femoral soft tissue during sideways falls. *Journal of Biomechanics,* , 110254.

Maitland, L. A., Myers, E. R., Hipp, J. A., Hayes, W. C., & Greenspan, S. L. (1993). Read my hips: Measuring trochanteric soft tissue thickness. *Calcified Tissue International, 52*(2), 85-89. doi:10.1007/bf00308313

Majumder, S., Roychowdhury, A., & Pal, S. (2008). Effects of trochanteric soft tissue thickness and hip impact velocity on hip fracture in sideways fall through 3D finite element simulations. *Journal of Biomechanics, 41*(13), 2834-2842. doi:10.1016/j.jbiomech.2008.07.001

Majumder, S., Roychowdhury, A., & Pal, S. (2013). Hip fracture and anthropometric variations: Dominance among trochanteric soft tissue thickness, body height and body weight during sideways fall. *Clinical Biomechanics (Bristol, Avon), 28*(9-10), 1034-1040. doi:10.1016/j.clinbiomech.2013.09.008

Majumder, S., Roychowdhury, A., & Pal, S. (2007). Simulation of hip fracture in sideways fall using a 3D finite element model of pelvis–femur–soft tissue complex with simplified representation of whole body. *Medical Engineering & Physics, 29*(10), 1167-1178.

Markowitz, J. (2011). Probe selection, machine controls and equipment. *Carmody KA, Moore CL, Feller-Copman D.Handbook of Critical Care and Emergency Ultrasound.USA: McGraw-Hill Medical,* , 25-38.

Martel, D. R., Levine, I. C., Pretty, S. P., & Laing, A. C. (2018). The influence of muscle activation on impact dynamics during lateral falls on the hip. *Journal of Biomechanics, 66*, 111-118. doi:S0021-9290(17)30607-3 [pii]

Martel, D. R., Lysy, M., & Laing, A. C. (2020). Predicting population level hip fracture risk: A novel hierarchical model incorporating probabilistic approaches and factor of risk principles. *Computer Methods in Biomechanics and Biomedical Engineering,* , 1-14.

McMeeken, J. M., Beith, I. D., Newham, D. J., Milligan, P., & Critchley, D. (2004). The relationship between EMG and change in thickness of transversus abdominis. *Clinical Biomechanics, 19*(4), 337-342.

Mendis, M. D., Wilson, S. J., Stanton, W., & Hides, J. A. (2010). Validity of real-time ultrasound imaging to measure anterior hip muscle size: A comparison with magnetic resonance imaging. *Journal of Orthopaedic & Sports Physical Therapy, 40*(9), 577-581.

Minns, R. J., Marsh, A. M., Chuck, A., & Todd, J. (2007). Are hip protectors correctly positioned in use? *Age and Ageing, 36*(2), 140-144. doi:afl186 [pii]

Morin, S., Lix, L. M., Azimaee, M., Metge, C., Majumdar, S. R., & Leslie, W. D. (2012). Institutionalization following incident non-traumatic fractures in community-dwelling men and women. *Osteoporosis International, 23*(9), 2381-2386.

Nankaku, M., Kanzaki, H., Tsuboyama, T., & Nakamura, T. (2005). Evaluation of hip fracture risk in relation to fall direction. *Osteoporosis International, 16*(11), 1315-1320.

Nasiri, M., & Luo, Y. (2016). Study of sex differences in the association between hip fracture risk and body parameters by DXA-based biomechanical modeling. *Bone, 90*, 90-98.

Nazrun, A. S., Tzar, M. N., Mokhtar, S. A., & Mohamed, I. N. (2014). A systematic review of the outcomes of osteoporotic fracture patients after hospital discharge: Morbidity, subsequent fractures, and mortality. *Therapeutics and Clinical Risk Management, 10*, 937-948. doi:10.2147/TCRM.S72456 [doi]

Nielson, C. M., Bouxsein, M. L., Freitas, S. S., Ensrud, K. E., Orwoll, E. S., & Osteoporotic Fractures in Men (MrOS) Research Group. (2009). Trochanteric soft tissue thickness and hip fracture in older men. *The Journal of Clinical Endocrinology and Metabolism, 94*(2), 491-496. doi:10.1210/jc.2008-1640

Nikitovic, M., Wodchis, W. P., Krahn, M. D., & Cadarette, S. M. (2013). Direct health-care costs attributed to hip fractures among seniors: A matched cohort study. *Osteoporosis International, 24*(2), 659-669.

Parachute. (2021). *The cost of injury in canada.* (). Toronto, ON: Parachute. Retrieved from https://parachute.ca/en/professional-resource/cost-of-injury-in-canada/

Pretty, S. P., Martel, D. R., & Laing, A. C. (2017). The influence of body mass index, sex, & muscle activation on pressure distribution during lateral falls on the hip. *Annals of Biomedical Engineering, 45*(12), 2775-2783. doi:10.1007/s10439-017-1928-z [doi]

Pretty, S. P., Levine, I. C., & Laing, A. C. (2021a). Anatomically aligned loading during falls: Influence of fall protocol, sex and trochanteric soft tissue thickness. *Annals of Biomedical Engineering, 49*(12), 3267-3279.

Pretty, S. P., Levine, I. C., & Laing, A. C. (2021b). Factors that influence the distribution of impact force relative to the proximal femur during lateral falls. *Journal of Biomechanics, 127*, 110679.

Public Health Agency of Canada. (2014). Seniors' falls in canada: Second report.

Pulkkinen, P., Eckstein, F., Lochmüller, E., Kuhn, V., & Jämsä, T. (2006). Association of geometric factors and failure load level with the distribution of cervical vs. trochanteric hip fractures. *Journal of Bone and Mineral Research, 21*(6), 895-901.

Roberts, B. J., Thrall, E., Muller, J. A., & Bouxsein, M. L. (2010). Comparison of hip fracture risk prediction by femoral aBMD to experimentally measured factor of risk. *Bone, 46*(3), 742-746.

Robinovitch, S. N., Evans, S. L., Minns, J., Laing, A. C., Kannus, P., Cripton, P. A., . . . Cameron, I. D. (2009). Hip protectors: Recommendations for biomechanical testing—an international consensus statement (part I). *Osteoporosis International, 20*(12), 1977-1988.

Robinovitch, S. N., Hayes, W. C., & McMahon, T. A. (1991). Prediction of femoral impact forces in falls on the hip. *Journal of Biomechanical Engineering, 113*(4), 366-374. doi:10.1115/1.2895414

Robinovitch, S. N., McMahon, T. A., & Hayes, W. C. (1995). Force attenuation in trochanteric soft tissues during impact from a fall. *Journal of Orthopaedic Research : Official Publication of the Orthopaedic Research Society, 13*(6), 956-962. doi:10.1002/jor.1100130621

Sarvi, M. N., & Luo, Y. (2015). A two-level subject-specific biomechanical model for improving

    prediction of hip fracture risk. *Clinical Biomechanics, 30*(8), 881-887.

Schacter, I., & Leslie, W. D. (2014). Estimation of trochanteric soft tissue thickness from dual-energy

    X-ray absorptiometry. *Journal of Clinical Densitometry : The Official Journal of the*

    International Society for Clinical Densitometry, 17(1), 54-59. doi:10.1016/j.jocd.2013.01.007

Schorr, M., Dichtel, L. E., Gerweck, A. V., Valera, R. D., Torriani, M., Miller, K. K., & Bredella, M.

    A. (2018). Sex differences in body composition and association with cardiometabolic risk.

    Biology of Sex Differences, 9, 1-10.

Scott, V., Wagar, L., & Elliot, S. (2010). *Falls and related injuries among older canadians: Fall-*

    related hospitalizations and intervention initiatives. prepared on behalf of the public health

    agency of canada, division of aging and seniors. ().

Tarride, J., Hopkins, R. B., Leslie, W. D., Morin, S., Adachi, J. D., Papaioannou, A., . . . Goeree, R.

    (2012). The burden of illness of osteoporosis in canada. *Osteoporosis International, 23*(11),

    2591-2600.

Thoirs, K. (2012). Physical and technical principles of sonography: A practical guide for non-

    sonographers. *Radiographer, 59*(4), 124-132.

Thoirs, K., & English, C. (2009). Ultrasound measures of muscle thickness: Intra-examiner reliability

    and influence of body position. *Clinical Physiology and Functional Imaging, 29*(6), 440-446.

Town, C. M., Gyemi, D. L., Ellis, Z., Kahelin, C., Laing, A. C., & Andrews, D. M.Predicting soft

    tissue thicknesses overlying the iliac crests and greater trochanters of younger and older adults.

    Submitted to Journal of Clinical Densitometry,

van Schoor, N. M., Van der Veen, A. J., Schaap, L. A., Smit, T. H., & Lips, P. (2006). Biomechanical

    comparison of hard and soft hip protectors, and the influence of soft tissue. *Bone, 39*(2), 401-

    407.

Weir, J. P. (2005). Quantifying test-retest reliability using the intraclass correlation coefficient and the

    SEM. *The Journal of Strength & Conditioning Research, 19*(1), 231-240.

Yang, Y., Komisar, V., Shishov, N., Lo, B., Korall, A. M., Feldman, F., & Robinovitch, S. N. (2020).

    The effect of fall biomechanics on risk for hip fracture in older adults: A cohort study of Video-

    Captured falls in Long-Term care. *Journal of Bone and Mineral Research,*

Appendix A– Comparison between Measurement Methods

Two methods of measuring soft tissue thickness were used to analyze the data collected in this thesis (Figure 4-1). Method 1: For all locations, thickness measurements were taken from the middle of the ultrasound image straight down to the underlying landmark of interest as the center of the probe was placed over the marked location on the participant's skin (Figure 4-1a). This method for measuring soft tissue thickness provides the thickness of the soft tissues lying directly under the measurement point on the skin. TST was measured from the skin surface in the middle of the image straight down to the underlying femur. MT was measured in the middle of the image from the outer edge of the muscle fascia to the outer edge of the femur. AT was measured from the middle of the image from the outer edge of the muscle fascia to the inner edge of the skin. Method 2: For all locations TST was measured from the skin marker (middle of the image corresponds to the marker on the skin) to the most superficial aspect of the femur. MT and AT were measured along the same plane as TST using the landmarks described previously (outer edge of femur to outer edge of fascia and outer edge of fascia to inner edge of skin) (Figure 4-1b).

Detailed results for method 1 were presented and discussed in sections 3.2 and 3.3 of this thesis. A comparison of method 1 and method 2 data is presented here. There were minimal differences in reliability for any of the measured soft tissue thicknesses between measurement locations (Figure 4-2). There were also minimal differences in thickness measurements for any of the tissues measured within both males and females combines as well as separate (Figure 4-3, Figure 4-4, and Figure 4-5).
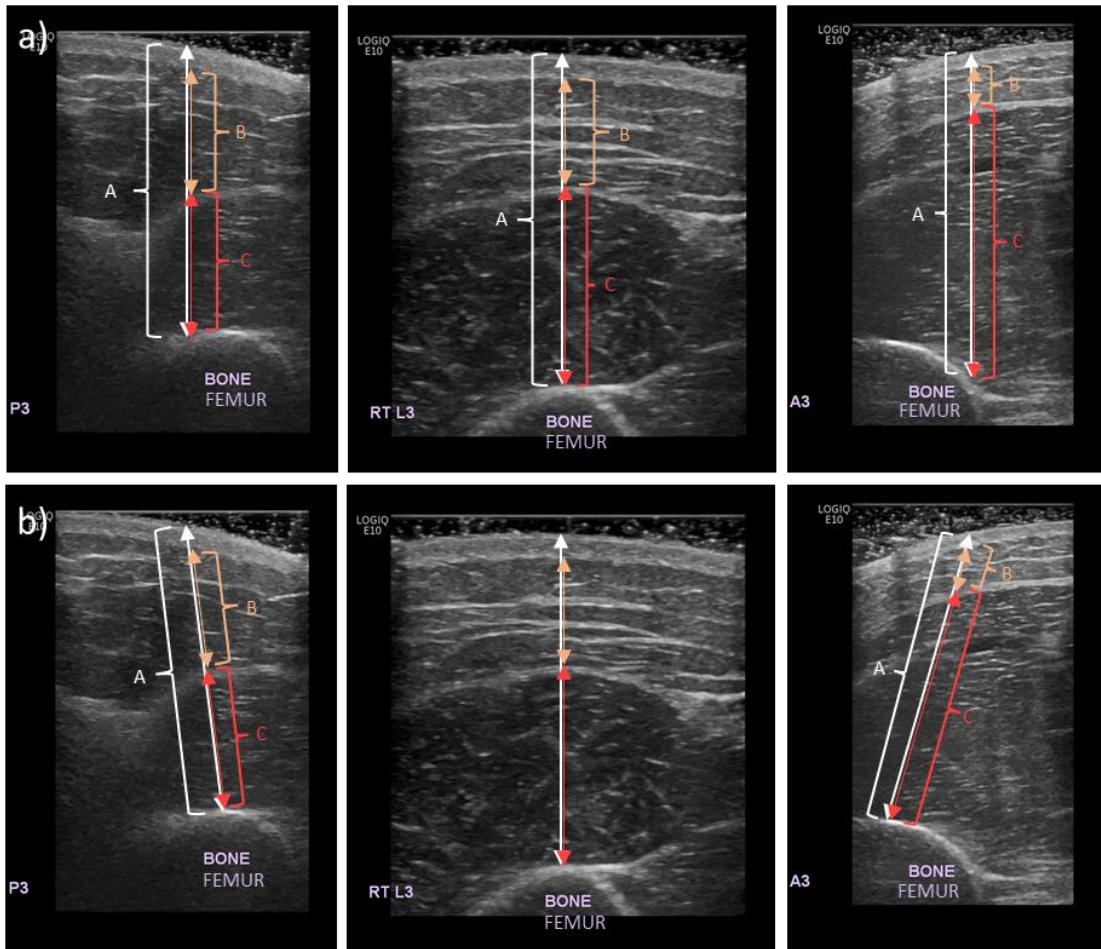
Figure 4-1: Transverse plane ultrasound images of P3, L3, and A3 measurement locations for both methods of measuring soft tissue thickness. Total soft tissue thickness is represented by the white arrow (A), subcutaneous adipose tissue thickness is represented by the orange arrow (B), and muscle thickness is represented by the red arrow (C). a) Demonstrates method 1 for measuring soft tissue thickness. All measurements are taken along the straight line directly underneath the skin surface marker. b) Demonstrates method 2 for measuring soft tissue thickness where TST is measured as the distance between the skin marker and the most superficial aspect of the femur. MT and AT are measured along the same plane as TST.
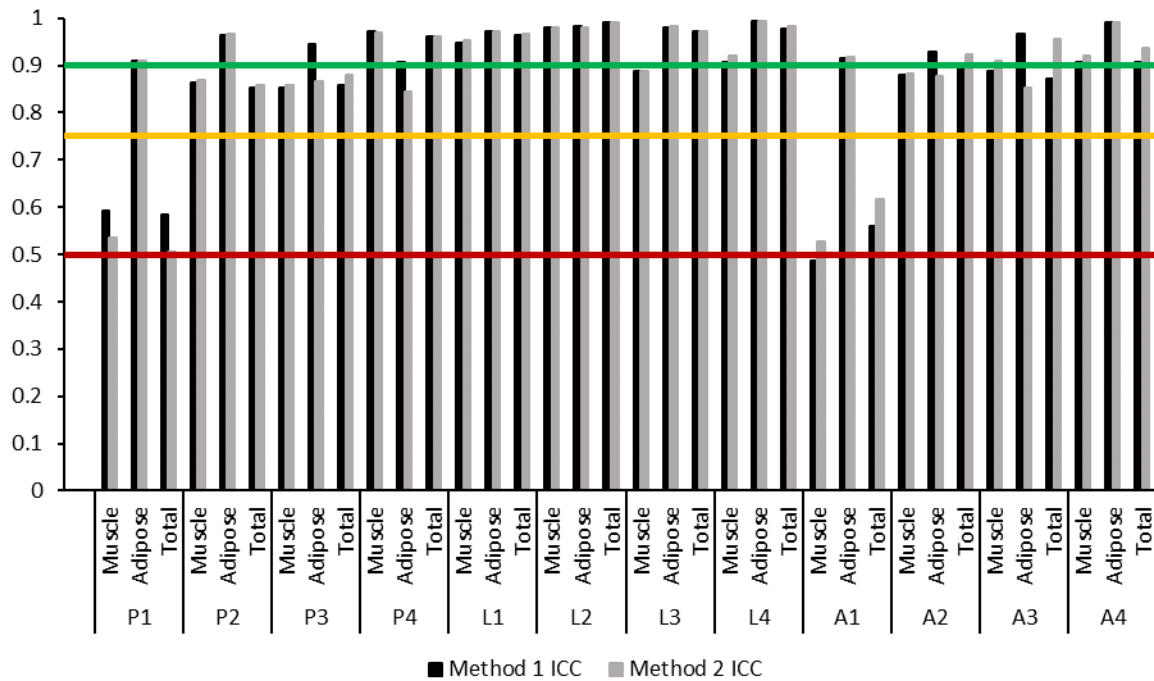
Figure 4-2: Comparison between ICCs calculated using data analyzed with method 1 and method 2 across all tissue types.
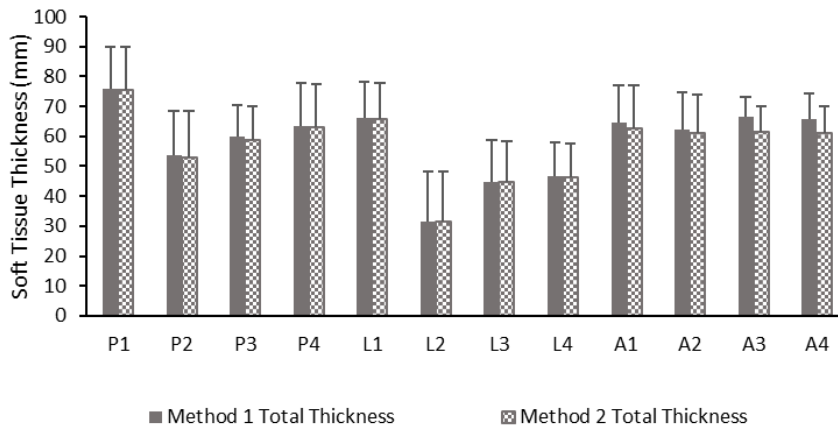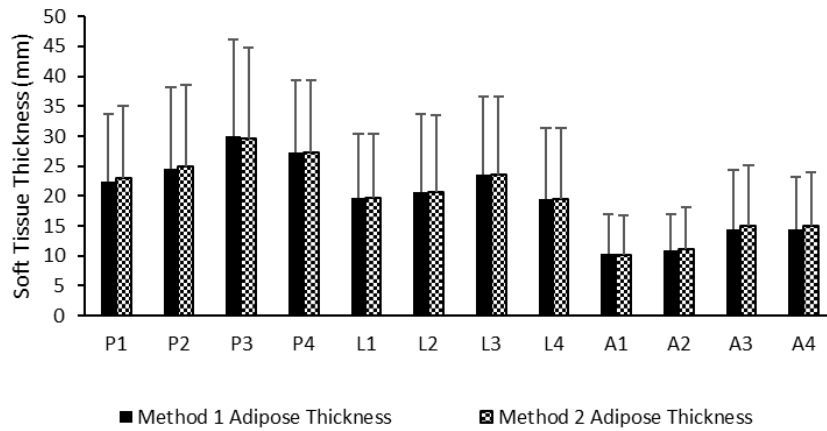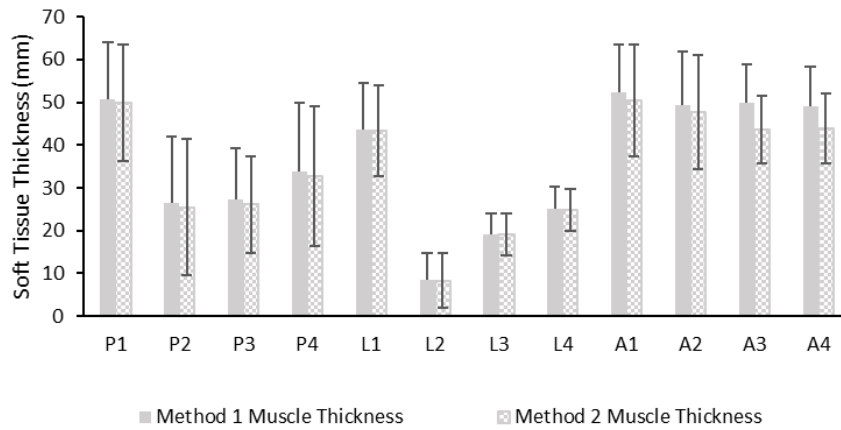
Figure 4-3: Comparison between measurement methods for muscle, adipose, and total soft tissue thickness measurements
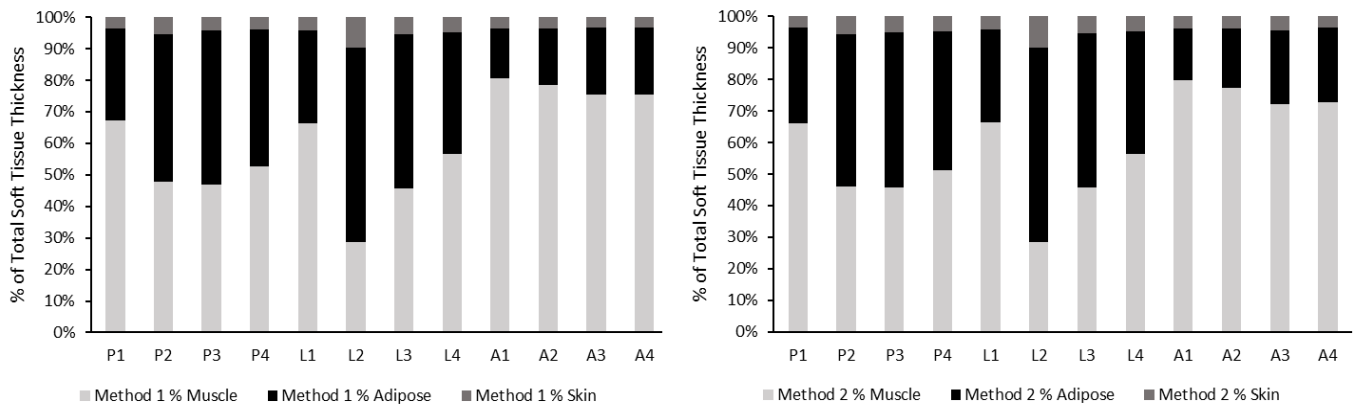
Figure 4-4: Comparison between measurement methods for the percent contribution of muscle, adipose, and skin to total soft tissue thickness.
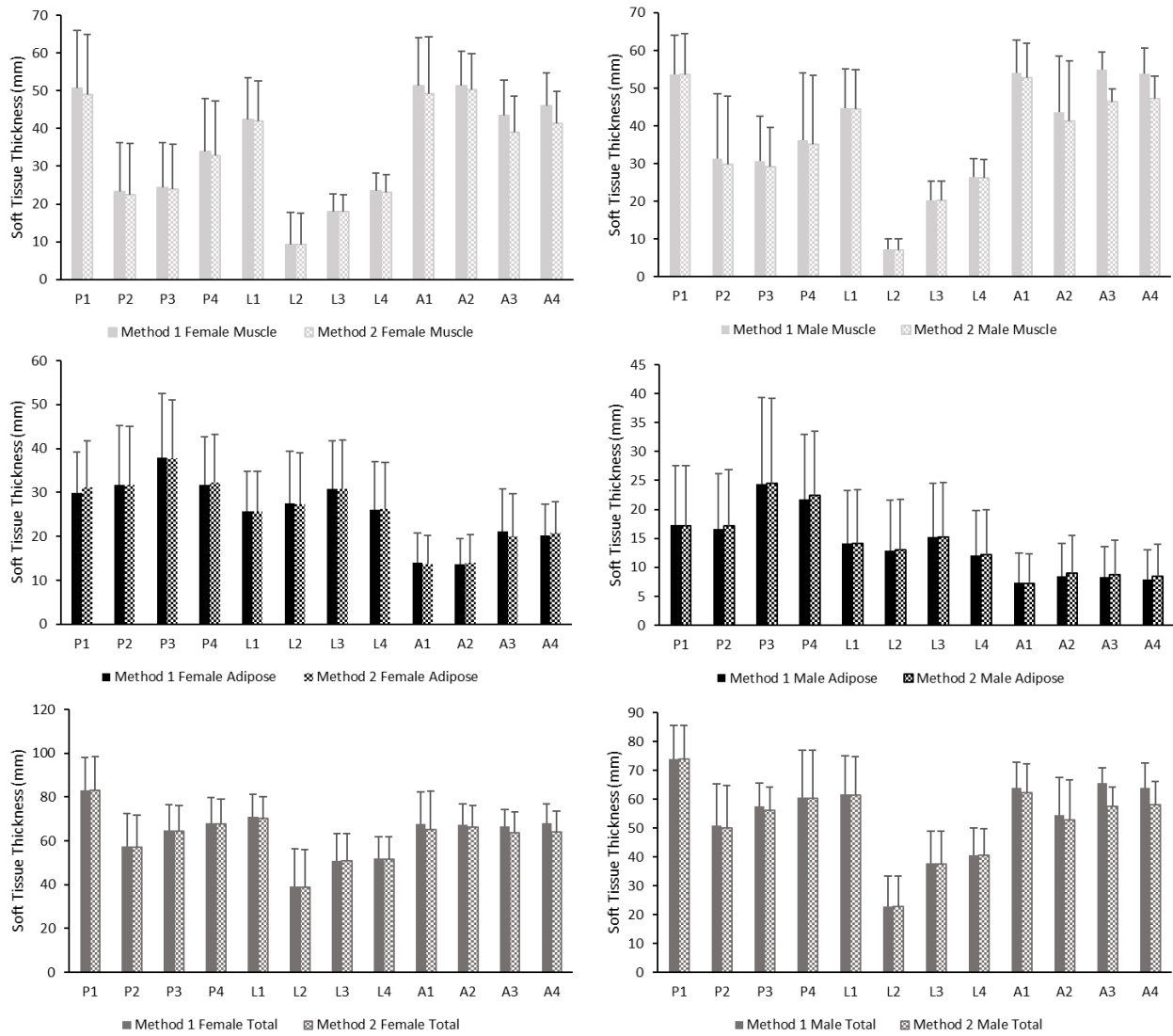
Figure 4-5: Comparison between method 1 and method 2 thickness measurements for each tissue type within females and males.

Appendix B – Intraclass Correlation Coefficients for Males and Females
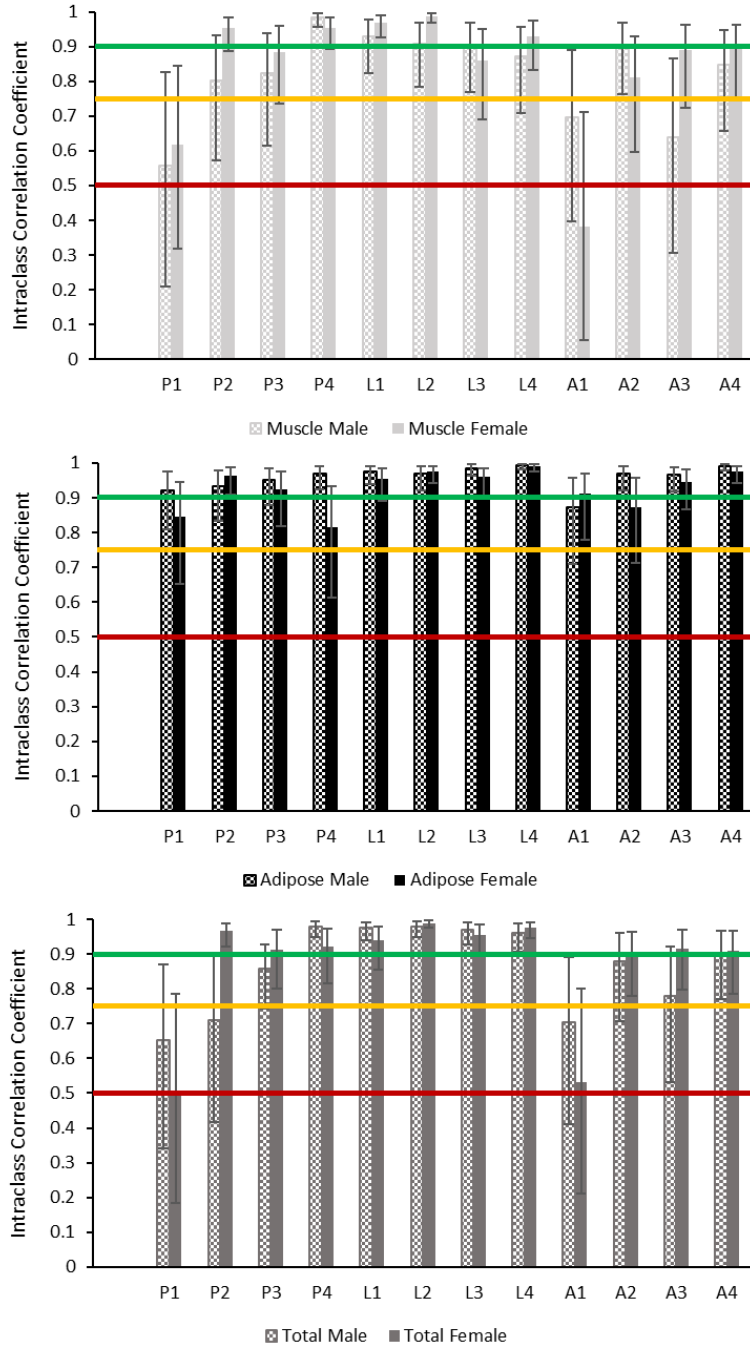
Figure 5-1: Comparison between ICCs calculated for males and females for muscle, adipose, and total soft tissues.

Appendix C – Developing the Protocol

During the piloting phase of this thesis, several initial methods for the collection were tried. Here, you will find a description of the methods that were tried, but did not work well, as part of the protocol development phase of the thesis.

1. <u>Participant positioning:</u> To simulate a sideways fall, I initially tried positioning participants on the table with their hips and knees flexed to a 45-degree angle to better represent the orientation a person would be in during a sideways fall (Nankaku et al., 2005; Yang et al., 2020). However, this orientation made it challenging to landmark and mark the measurement grid on participants (as the grid needed to be aligned along the femur diaphysis). The challenge was that I was unable to see anatomical landmarks such as the iliac crest, the ASIS, and the lateral condyle of the knee. To get around these difficulties, I decided to have participants position their hips and knees straight, with no flexion.

2. <u>Landmarking the GT:</u> Initially, I tried to locate and mark the GT while participants were on the table in the side-lying position. This was challenging as once again I was unable to see anatomical landmarks to help guide me to the GT. Additionally, I was unable to ask participants to internally and externally rotate their hip (i.e. squish a bug) to assist with palpation of the GT. Finally, I discovered that indelible ink does not write well through ultrasound gel (even after the gel was wiped off the participant). Therefore, only using the ultrasound to locate the GT was not feasible. To get around these difficulties, I decided to palpate and mark the GT while participants were standing, and then use the ultrasound to confirm the GT placement once participants were on the table.

3. <u>Obtaining good visualization of the femur, muscle, adipose, and skin in the off-axis locations (P1 – P4 and A1 – A4):</u> Initially I tried to keep the ultrasound perpendicular to the skin surface along both the long and short axis of the femur. However, when I did this, it was next to impossible to visualize the femur as most of the ultrasound waves were not hitting the bone. I found that tilting the probe anteriorly or posteriorly (along the short axis of the femur), while keeping it perpendicular to the long axis of the femur, allowed the ultrasound waves to hit the femur and echo back to the probe, thereby allowing me to visualize both the femur and the soft tissues at the off-axis locations.

4. <u>Probe type:</u> Initially I wanted to collect participants across the range of BMIs (low – obese). Doing so would have required the use of a curvilinear probe to ensure that I had enough

penetration depth to image individuals with more than 14 cm of total soft tissue thickness. However, I found when piloting that differentiating between the muscle and adipose tissues became more challenging with the curvilinear probe (due to the lower image resolution). Because of this, I decided to use a linear probe and only collect participants with self-reported low to normal BMI.